Electronic Supplementary Material (ESI) for Polymer Chemistry.

Supporting Information

Increased block copolymer length improves intracellular availability of protein cargo

Christopher R. Hango,[†] Hazel C. Davis,[†] Esha A. Uddin,[†] Lisa M. Minter,[‡,§] and Gregory N. Tew[*,†,‡,§]

[†]*Department of Polymer Science & Engineering, University of Massachusetts, Amherst, Massachusetts 01003, United States*

[‡]*Molecular and Cellular Biology Program, University of Massachusetts, Amherst, Massachusetts 01003, United States*

[§]*Department of Veterinary & Animal Sciences, University of Massachusetts, Amherst, Massachusetts 01003, Untied States*

**Email: tew@mail.pse.umass.edu*

Table of Contents

I. Materials S3
A. Synthesis S3
B. Protein Cargoes S3
C. Reporter Jurkat T Cell Line S4
D. Cell Culture Reagents S4
II. Instrumentation and Software S5
Methods S7
A. Synthesis S7
1. Monomer Synthesis S7
2. Polymer Synthesis S11
3. Polymer Deprotection S19
B. Protein Delivery S19
1. Homopolymer-Mediated EGFP Delivery S19
2. Block Copolymer-Mediated EGFP Delivery S20
3. Block Copolymer-Mediated IgG Delivery in Jurkat T Cells S21
4. Block Copolymer-Mediated IgG Delivery in mHippoE-18 Cells S21
5. Cre Delivery: PTDM Molecular Weight Comparison S22
6. Cre Delivery: PTDM Molar Ratio Comparison S23
C. Dynamic Light Scattering S23
D. Fluorescence-Based Equilibrium Binding Assays S25
III. Supplemental Data S26
A. IgG-AF488 Delivery in mHippoE-18 Cells S26
B. Cellular Viability S27
C. Impact of Block Copolymer Length on Binding S31
D. Particle Size by Dynamic Light Scattering S32
1. DLS of PTDM:IgG Complexes S32
2. DLS of PTDM:Cre Complexes S37
IV. References S40

I. Materials

A. Synthesis

Chemicals and solvents were obtained as reagent grade from Millipore Sigma, Alfa Aesar, Fisher Scientific, Fluka, BDH, or Acros Organics and used as received unless otherwise noted. Grubbs 3rd generation catalyst (Dichloro-di(3-bromopyridino)-N,N'-Dimesitylenoimidazolino-Ru=CHPh; G3) was synthesized as described previously.[1] Deuterated NMR solvents were obtained from Cambridge Isotope Laboratories. Polymers were dialyzed using Spectra/Por® dialysis membranes with molecular weight cutoffs (MWCOs) ranging from 0.5-1 kDa.

B. Protein Cargoes

Recombinant enhanced green fluorescent protein (EGFP) with both an N-terminal and a C-terminal 6XHis tag was purchased from BioVision (product code 4999), reconstituted to a concentration of 1 mg/mL in 1x PBS, and stored at -20 °C, per manufacturer recommendations.

Cross-adsorbed goat anti-rabbit immunoglobulin G, fluorescently labelled with Alexa Fluor 488 (herein referred to as "IgG-AF488"), was purchased from ThermoFisher Scientific (product number A-11008) and stored in the dark at 4 °C upon receipt, per manufacturer recommendations.

Bovine serum albumin fluorescently labelled with fluorescein isothiocyanate (herein referred to as "BSA-FITC") was purchased from Millipore Sigma (product number A9771) and stored in the dark at 4 °C upon receipt, per manufacturer recommendations.

Unlabeled immunoglobulin G from goat serum (herein referred to as "IgG") was purchased from Millipore Sigma (product number I5256) and stored at 4 °C upon receipt, per manufacturer recommendations.

Recombinant Cre recombinase with an N-terminal 6XHis tag and NLS sequence (PKKKRKV) was purchased from Excellgen (HNC form, old product code RP-7, new product code EG-1067) and stored at -20 °C, per manufacturer recommendations.

C. Reporter Jurkat T Cell Line

The Jurkat reporter cell line (herein referred to as "Jurkat-GFP") was created by stably transfecting Jurkat T cells with the pWPT-GFP plasmid. pWPT-GFP was a gift from Didier Trono (Addgene plasmid # 12255; http://n2t.net/addgene:12255; RRID:Addgene_12255). A single cell containing one copy of the *EGFP* gene was then identified, isolated, and expanded to create the monoclonal cell line used for Cre delivery.

D. Cell Culture Reagents

Jurkat T cells and the modified Jurkat-GFP cell line were cultured in Gibco™ RPMI 1640 High Glucose GlutaMAX™ Supplement (Thermo Fisher Scientific), supplemented with 10% (v/v) EquaFETAL (Atlas Biologicals), 1% (v/v) 100 mM Sodium Pyruvate Solution (Lonza) or 100 mM HyClone™ Sodium Pyruvate Solution (Fisher Scientific), 1% (v/v) 100x MEM Non-Essential Amino Acid Solution (Lonza) or 100x HyClone™ Non-Essential Amino Acids NEAA (Fisher Scientific), 1% (v/v) HEPES (1 M) (Thermo Fisher Scientific), and 1% (v/v) Penicillin-Streptomycin Mixture (10K/10K) (Lonza). Serum-free RPMI was formulated in the same manner, withholding the 10% EquaFETAL. Gibco™ 10X phosphate-buffered saline (PBS), pH 7.4 was

diluted to 1X prior to use. The embryonic mouse hippocampal-18 (mHippoE) cell line was cultured in Gibco™ DMEM High Glucose GlutaMAX™ Supplement (Thermo Fisher Scientific), supplemented with 10% (v/v) FBS or EquaFETAL (Atlas Biologicals), 1% (v/v) 100 mM Sodium Pyruvate Solution (Lonza) or 100 mM HyClone™ Sodium Pyruvate Solution (Fisher Scientific), 1% (v/v) 100x MEM Non-Essential Amino Acid Solution (Lonza) or 100x HyClone™ Non-Essential Amino Acids NEAA (Fisher Scientific), and 1% (v/v) Penicillin-Streptomycin Mixture (10LK/10K) (Lonza). Heparin sodium salt from porcine intestinal mucosa (≥100 IU/mg) (Alfa Aesar/VWR) was used to remove extracellular complexes from the cell surfaces. 7-aminoactinomycin D (7-AAD) Staining Solution (BD Biosciences/Fisher Scientific) was used to assess cellular viability in flow cytometry experiments. Bovine serum albumin, standard heat shock (Rocky Mountain Biologicals, Inc.) was used in FACS buffer preparation.

II. Instrumentation and Software

^{1}H nuclear magnetic resonance spectra were recorded for all monomers and polymers at 500 MHz using a Bruker Ascend Nuclear Magnetic Resonance Spectrometer retrofitted with a cryoprobe. Chemical shifts (δ) are listed in ppm and coupling constants (*J*) in Hz. Splitting patterns were described as either s, singlet; d, doublet; dd, doublet of doublets; t, triplet; tt triplet of triplets; dt, doublet of triplets; q, quartet; or m, multiplet; or br, broad. Analysis of NMR spectra was performed using MestReNova v. 6.1.0-6224 (Mestrelab Research).

Gel permeation chromatography (GPC) chromatograms were recorded for all polymers using an Agilent Technologies 1260 Infinity series system equipped with refractive index (RI) and ultraviolet (UV) detectors, a PL Gel 5 μm guard column, two PL Gel 5 μm analytical Mixed-C columns, and a PL Gel 5 μm analytical Mixed-D column. These columns were connected in series

and incubated at 40 °C. THF was used as the eluent at a flow rate of 1 mL/min. Toluene was used as the flow marker. The instrument was calibrated with both poly(methyl methacrylate) and polystyrene standards. All samples were prepared at ~3 mg/mL and filtered into Agilent Technologies autosampler vials using 0.45 μm PTFE syringe filters prior to injection.

Flow cytometry experiments were conducted using a BD Dual LSRFortessa™ flow cytometer and FACSDiva acquisition software. EGFP, AF488, and 7-AAD were all excited with a 488 nm laser. Fluorescence emission was collected using 530/30 (for EGFP and 7-AAD) and 710/50 band pass filters. Fluorescence signals were recorded for 10,000 cells in all samples. Analysis was performed using FlowJo v. 10.0.7r2 (Tree Star).

Fluorescence data for equilibrium binding assays were collected using a BioTek Instruments Synergy Mx plate reader and Gen5 1.10 acquisition software. Samples were measured at 25 °C in Ultra Cruz 96 well sterile poly(styrene) black tissue culture plates with clear flat bottoms purchased from Santa Cruz Biotechnology, Inc.

Dynamic light scattering experiments were conducted using a Malvern Instruments Zetasizer Nano Series Nano-ZS and Zetasizer software (v. 8.00.4813) for analysis. The standard operating procedure (SOP) used for all DLS experiments included the use of the instrument default "protein" as the material with a refractive index (RI) of 1.450 and absorption of 0.001. The dispersant selected in the SOP was a "complex solvent", 1x PBS, (RI = 1.3317, viscosity = 0.9051 cP), where the primary component selected was water and the minor components consisted of sodium chloride (0.1551 M), sodium phosphate dibasic (0.0030 M), and potassium bicarbonate (0.0010 M) as a substitute for potassium phosphate monobasic, which was the actual component in the 1x PBS used. Measurement temperature was set at 25°C with an equilibration time of 120 seconds

between measurements. The disposable cuvette option DTS0012 (for PTDM:IgG samples) or ZEN0040 (for PTDM:Cre samples) was also selected in the SOP. Light scattering was measured at a back-scattering angle of 173° with the number of runs per measurement set to automatic, 11 runs per measurement, and a run duration of 10 seconds. Each DLS trial consisted of 3 measurements. Finally, for data processing, the analysis model was a general purpose (normal resolution) model. Disposable polystyrene cuvettes with a volume capacity of 4.5 mL or 1.5 mL were purchased from Fisher Scientific. Poly(ethersulfone) (PES) syringe filters were purchased from the Restek Corporation.

Methods

A. Synthesis

The **PGON$_n$** and **dG$_n$** series of carriers studied have been previously characterized.[2,3] Although the **MePh$_{10}$-*b*-dG$_5$** carrier has also been reported previously, it was resynthesized for these studies. The following carriers are reported here for the first time: **MePh$_{20}$-*b*-dG$_{10}$**, **MePh$_{30}$-*b*-dG$_{15}$**, **MePh$_{40}$-*b*-dG$_{20}$**, and **MePh$_{80}$-*b*-dG$_{40}$**. Synthetic protocols and characterization data for the **MePh$_{2n}$-*b*-dG$_n$** series and its constituent monomers are detailed in the subsequent sections.

1. Monomer Synthesis

In general, the **dG** and **MePh** monomers were prepared following previously reported procedures.[4] A brief overview is provided here.

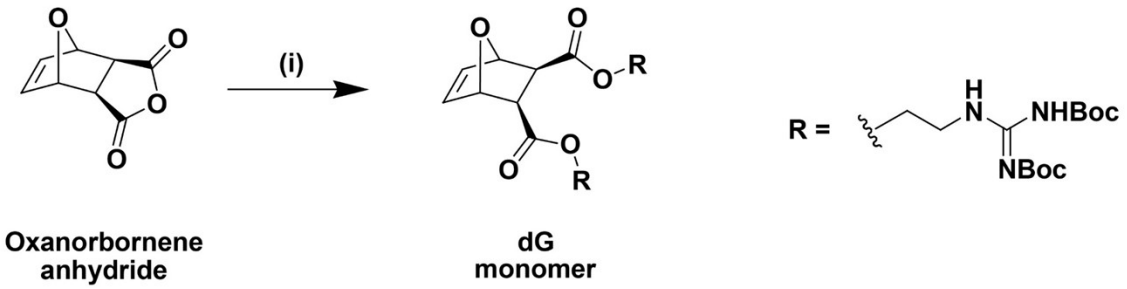

Figure S1: Synthesis of the symmetric **dG** monomer. (i) R-OH, DMAP, EDC, CH_2Cl_2, 0 °C to room temperature, overnight.

dG monomer: One molar equivalent of oxanorbornene anhydride, two molar equivalents of 1,3,-di-boc-2-(2-hydroxyethyl)guanidine, and 0.1 molar equivalents of DMAP were dissolved in freshly distilled CH_2Cl_2 dried over CaH_2 and stirred at room temperature under nitrogen. The solution was then cooled down to 0 °C in an ice bath and 1.2 molar equivalents of EDC were added. The solution was allowed to stir overnight under nitrogen and gradually return to room temperature. The diester product was isolated by normal phase flash chromatography using silica using a 70/30 (v/v) mixture of CH_2Cl_2/ethyl acetate (EtOAc) as the eluent. Pure fractions were combined and concentrated using rotary evaporation. The sample was dried under vacuum overnight at room temperature to obtain a white solid. The ^{1}H NMR spectrum of this molecule can be found in Figure S2.

71% yield

^{1}H NMR (500 MHz, $CDCl_3$) δ 11.49 (br, 2H), 8.56 (br, 2H), 6.47 (br, 2H), 5.35 – 5.27 (m, 2H), 4.33 – 4.19 (m, 4H), 3.83 – 3.61 (m, 4H), 2.85 (br, 2H), 1.69 – 1.39 (m, 36H).

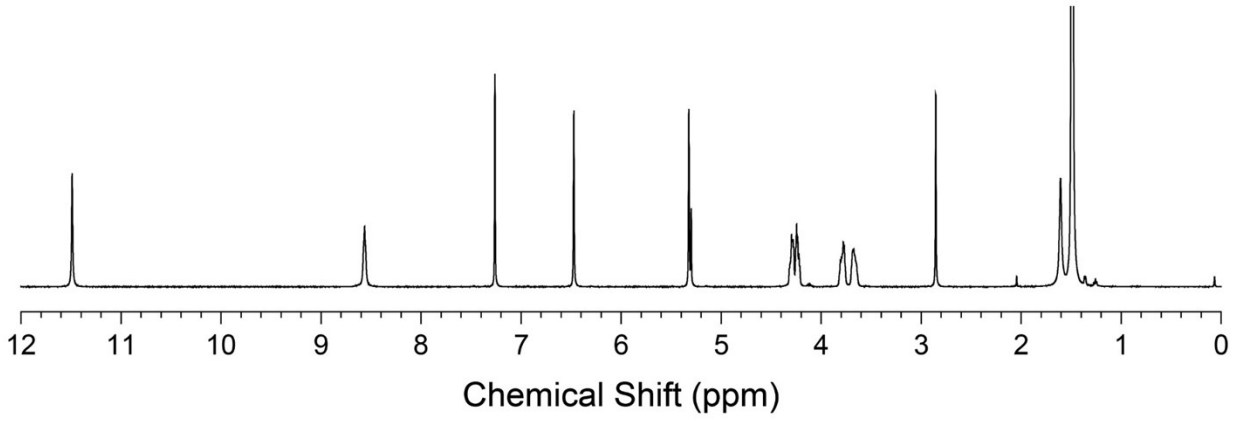

Figure S2: ^{1}H NMR spectrum in deuterated chloroform of the Boc-protected **dG** monomer after purification by flash chromatography.

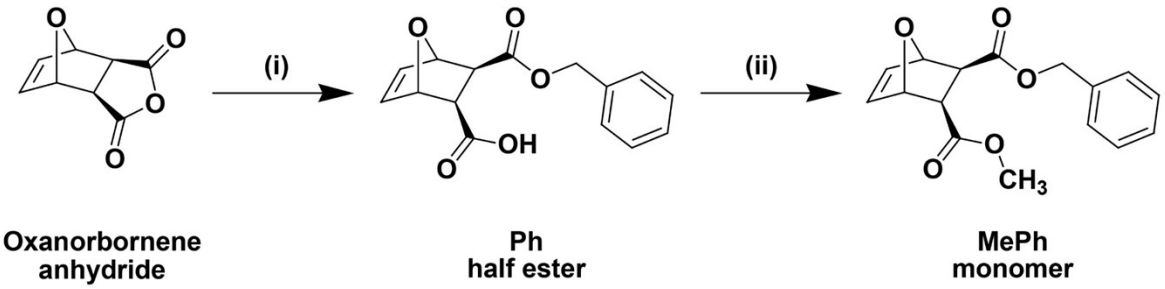

Figure S3: Synthesis of the asymmetric **MePh** monomer. (i) Methanol, DMAP, CH_2Cl_2, room temperature, overnight; (ii) benzyl alcohol, DMAP, EDC, CH_2Cl_2, 0 °C to room temperature, overnight.

Ph half ester: One molar equivalent of **oxanorbornene anhydride** and 0.1 molar equivalents of 4-dimethylaminopyridine (DMAP) were added to an oven dried two-neck round bottom flask under nitrogen gas and dissolved in sufficient freshly distilled CH_2Cl_2 dried over CaH_2. One molar equivalent of benzyl alcohol was added via syringe. The reaction was stirred overnight under nitrogen at room temperature. As the half ester product formed, it precipitated out overnight. The precipitate was isolated by vacuum filtration, washing with cold CH_2Cl_2, and then dried under vacuum. The ^{1}H NMR spectrum of this molecule can be found in Figure S4.

56% yield

^{1}H NMR (500 MHz, DMSO) δ 12.45 (s, 1H), 7.41 – 7.28 (m, 5H), 6.50 – 6.42 (m, 2H), 5.11 (d, *J* = 5.8 Hz, 2H), 5.08 – 4.91 (m, 2H), 2.81 – 2.73 (m, 2H).

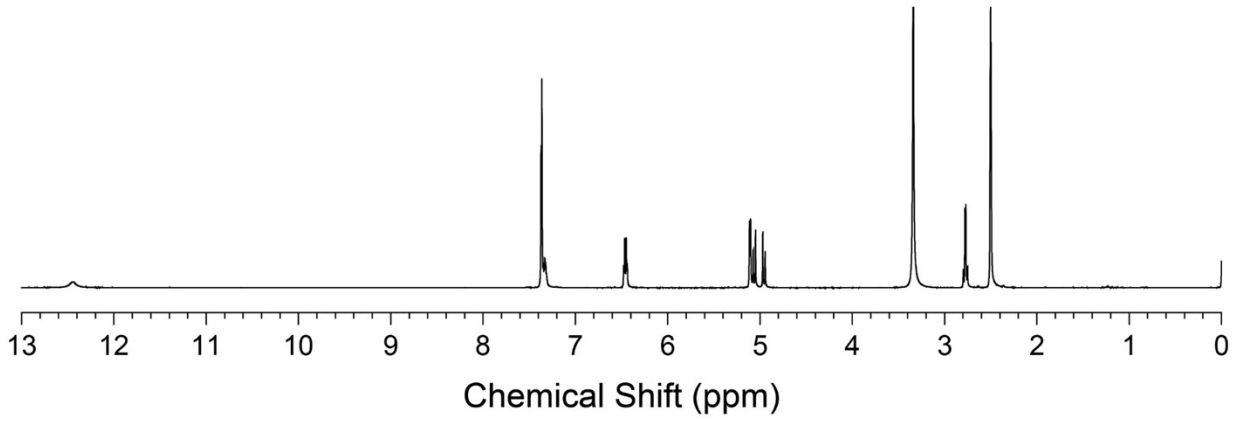

Figure S4: ^{1}H NMR spectrum in deuterated dimethyl sulfoxide of the Boc-protected **Ph half ester** monomer precursor after purification by vacuum filtration.

MePh monomer: One molar equivalent of the **Ph half ester** and 0.1 molar equivalents of DMAP were added to an oven dried two-neck round bottom flask under nitrogen gas and dissolved in sufficient freshly distilled CH_2Cl_2 dried over CaH_2. One molar equivalent of methanol was added via syringe. The solution was then cooled down to 0 °C in an ice bath and 1.2 molar equivalents of 1-ethyl-3-(3-dimethylaminopropyl)carbodiimide (EDC) were added. The solution was allowed to stir overnight under nitrogen and gradually return to room temperature. The diester product was isolated by normal phase flash chromatography with silica using a 90/10 (v/v) mixture of CH_2Cl_2/EtOAc as the eluent. Pure fractions were combined and concentrated using rotary evaporation. The sample was dried under vacuum overnight at room temperature to obtain a white solid. The ^{1}H NMR spectrum of this molecule can be found in Figure S5**Figure S2**.

69% yield

^{1}H NMR (500 MHz, $CDCl_3$) δ 7.40 – 7.29 (m, 5H), 6.47 – 6.42 (m, 2H), 5.28 (d, J = 3.4 Hz, 2H), 5.18 – 5.10 (m, 2H), 3.55 (s, 3H), 2.88 – 2.79 (m, 2H).

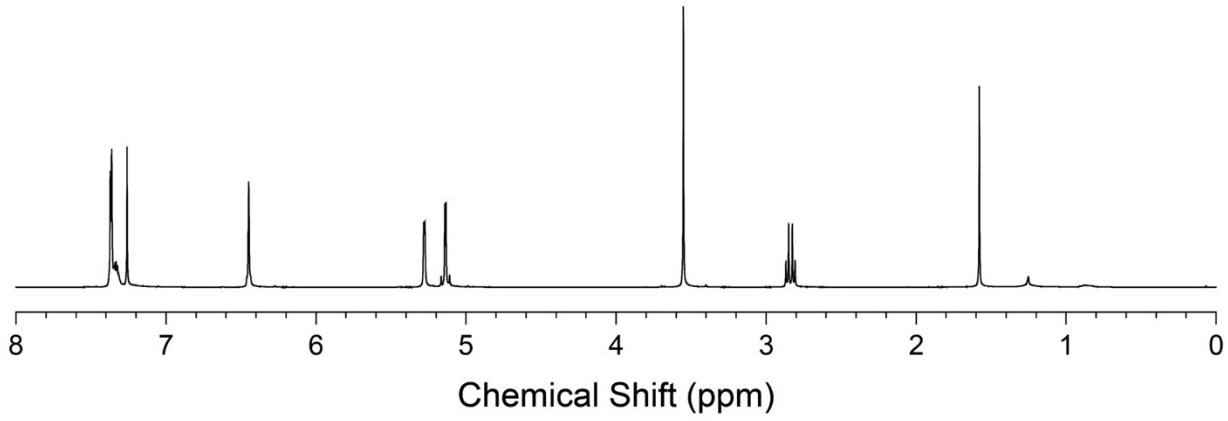

Figure S5: ^{1}H NMR spectrum in deuterated chloroform of the **MePh** monomer after purification by flash chromatography.

2. Polymer Synthesis

All polymers were prepared according to previously reported procedures.[4]

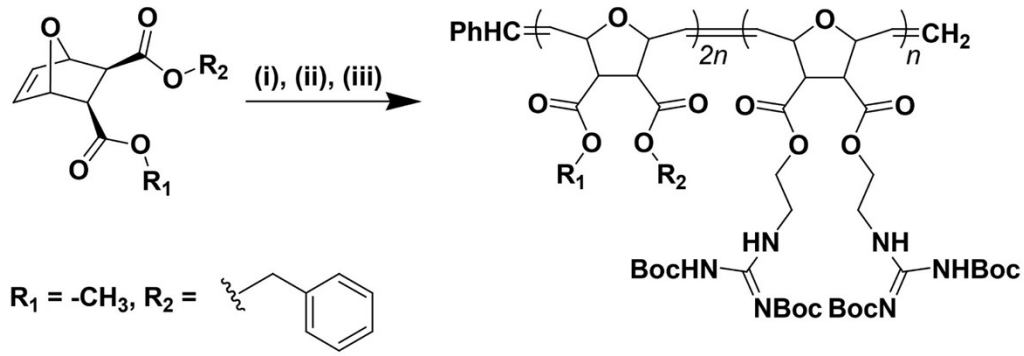

Figure S6: Synthesis of Boc-protected block copolymers. (i) G3, CH_2Cl_2, room temperature, 10 min; (ii) **dG**, CH_2Cl_2, room temperature, 90 min; (iii) ethyl vinyl ether, room temperature, overnight.

In brief, 1 molar equivalent of G3, 10-80 molar equivalents of the **MePh** monomer (depending on the target length of the hydrophobic block), and 5-40 molar equivalents of the **dG** monomer (depending on the target length of the cationic block) were each dissolved in separate oven dried Schlenk flasks using freshly distilled CH_2Cl_2 dried over CaH_2. The contents of all Schlenk flasks were put through a minimum of 3 freeze, pump, thaw (FPT) cycles to rigorously degas the monomer and catalyst solutions. After the final FPT cycle, the contents of the flask containing the

hydrophobic monomer were cannulated into the flask containing the stirring G3 solution. This monomer was allowed to polymerize for about 10 minutes, at which time a crude aliquot was taken and dried using compressed air for analysis by ^{1}H NMR and THF GPC. The NMR spectrum was used to confirm monomer consumption by a complete upfield shift of the alkene protons in the oxanorbornene-based monomer. The GPC chromatogram was used to calculate the molecular weight and dispersity of the hydrophobic block. The **dG** monomer was then cannulated into the G3 flask and allowed to polymerize for approximately 90 minutes. Upon completion, 2-3 mL of ethyl vinyl ether (EVE) was injected into the Schlenk flask to terminate the polymerization. A crude aliquot was taken at this point and dried using compressed air for analysis by ^{1}H NMR and THF GPC. As with the first aliquot, this NMR spectrum was used to confirm complete consumption of the second monomer. The GPC chromatogram was used to confirm successful chain extension by comparison with the first chromatogram. After stirring overnight with EVE, the crude reaction mixture was concentrated to a solid using rotary evaporation before it was redissolved in 1 mL of tetrahydrofuran (THF). This solution was then precipitated dropwise into cold, stirring pentane. The precipitated polymers in their Boc-protected forms were recovered using vacuum filtration and dried under high vacuum overnight, at which point they were again characterized by ^{1}H NMR and THF GPC. The final NMR spectrum was used to calculate the relative block composition using integrations of diagnostic peaks from each of the respective blocks (Table S1). For this analysis, the oxanorbornene backbone -CH protons at ~3.15-3.13 ppm were compared to the **dG** block -CH_2 protons at ~4.22-4.16 ppm. The final GPC chromatogram was used to determine the molecular weight (MW) averages and dispersity (Đ) of each polymer, reported in Table S1.

Table S1: Polymer characterization summary from ^{1}H NMR and THF GPC analysis.

Polymer	**Block 1:**	**Theoretical**	**M_p**	**M_n**	**M_w**	**Đ[c]**

	Block 2[a]	MW (kDa)[b]	(kDa)[c]	(kDa)[c]	(kDa)[c]	
PGON$_{20}$[d]	--	9.11	11.2	9.56	10.5	1.10
PGON$_{40}$[d]	--	18.1	19.0	17.3	18.4	1.05
PGON$_{80}$[d]	--	36.1	44.2	34.4	38.4	1.12
dG$_{20}$[d]	--	15.2	13.5	12.7	13.4	1.06
dG$_{40}$[d]	--	30.3	30.5	23.6	27.2	1.15
dG$_{80}$[d]	--	60.5	71.0	50.2	59.2	1.18
MePh$_{10}$-*b*-dG$_5$	67:33	6.76	7.73	6.65	7.39	1.11
MePh$_{20}$-*b*-dG$_{10}$	69:31	13.4	15.4	12.4	14.2	1.14
MePh$_{30}$-*b*-dG$_{15}$	69:31	20.1	22.2	17.6	20.2	1.15
MePh$_{40}$-*b*-dG$_{20}$	68:32	26.7	27.3	23.0	25.1	1.09
MePh$_{80}$-*b*-dG$_{40}$	68:32	53.4	54.2	40.3	46.9	1.16

[a]Relative block incorporation as calculated by ^{1}H NMR. [b]Theoretical molecular weight based on polymer structure shown in Figure S6. [c]Calculated by GPC in THF, 40 °C, flow rate 1 mL/min with polystyrene (**PGON$_n$** and **MePh$_{2n}$-*b*-dG$_n$**) or poly(methyl methacrylate) (**dG$_n$**) standards and toluene as the flow marker. [d]Data summarized from previous reports.[2,3]

The ^{1}H NMR chemical shifts for each precipitated, Boc-protected polymer are below, and the corresponding spectra can be found in Figure S7, Figure S9, Figure S11, Figure S13, and Figure S15. Overlays of the intermediate and final GPC chromatograms taken for each polymer can be found in Figure S8, Figure S10, Figure S12, Figure S14, and Figure S16. An overlay of the final chromatograms for all block copolymers can be found in Figure S17.

MePh$_{10}$-*b*-dG$_5$: ^{1}H NMR (500 MHz, CD_3CN) δ 11.52 (br, 2H), 8.35 (br, 2H), 7.34 (br, 10H), 5.84 (*trans*) and 5.59 (*cis*) (br, 6H total), 5.09 (br, 4H), 5.09 (*cis*) and 4.62 (*trans*) (br, 6H total), 4.22 (br, 4H), 3.55 (br, 4H), 3.47 (br, 6H), 3.13 (br, 6H), 1.47 (s, 18H), 1.41 (s, 18H).

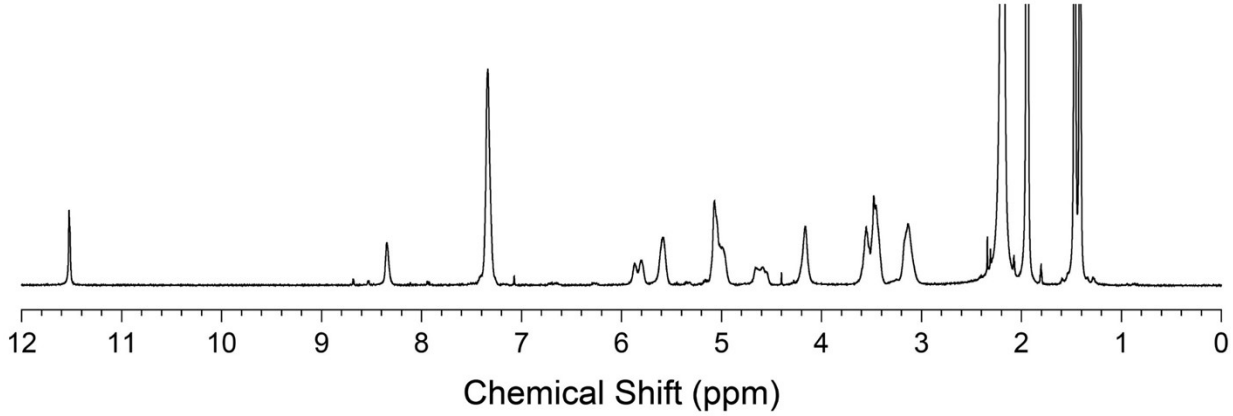

Figure S7: ^{1}H NMR spectrum in deuterated acetonitrile of the Boc-protected copolymer **MePh$_{10}$-*b*-dG$_5$** after purification by precipitation.

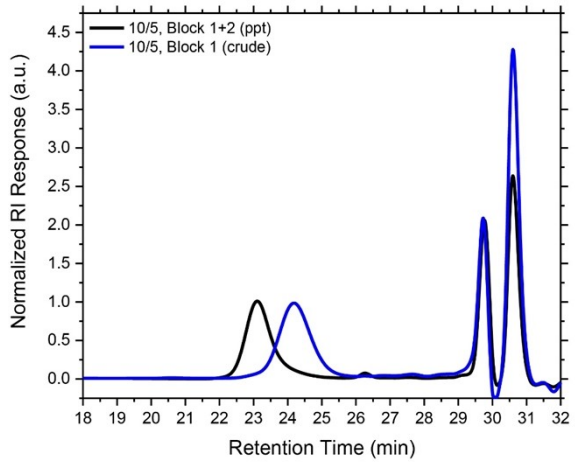

Figure S8: GPC traces illustrating the increase in molecular weight upon chain extension of the first block (containing just the **MePh** monomer) to create the Boc-protected copolymer (**MePh$_{10}$-*b*-dG$_5$**), shown here after purification by precipitation.

MePh$_{20}$-*b*-dG$_{10}$: ^{1}H NMR (500 MHz, CD_3CN) δ 11.53 (br, 2H), 8.35 (br, 2H), 7.33 (br, 10H), 5.84 (*trans*) and 5.58 (*cis*) (br, 6H total), 5.03 (br, 4H), 5.03 (*cis*) and 4.60 (*trans*) (6H total), 4.16 (br, 4H), 3.55 (br, 4H), 3.46 (br, 6H), 3.13 (br, 6H), 1.47 (s, 18H), 1.41 (s, 18H).

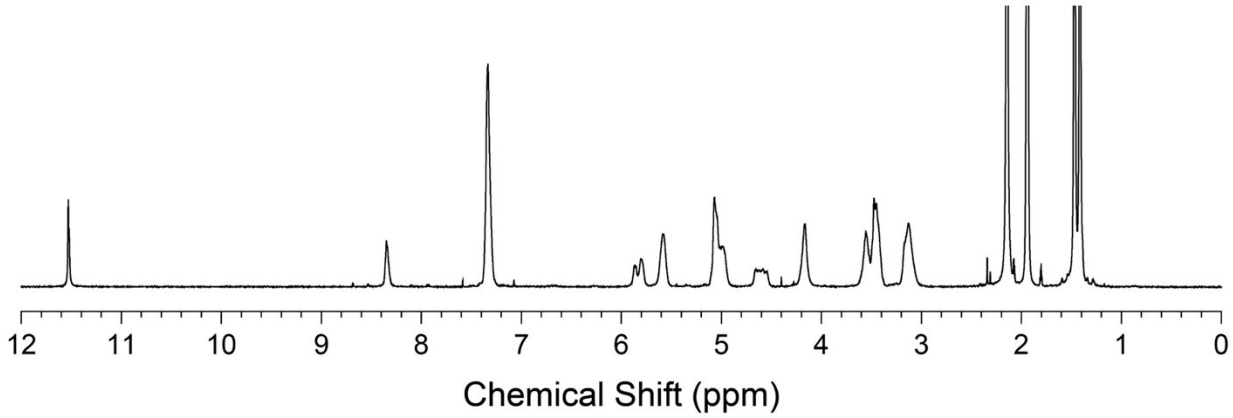

Figure S9: ^{1}H NMR spectrum in deuterated acetonitrile of the Boc-protected copolymer **MePh$_{20}$-*b*-dG$_{10}$** after purification by precipitation.

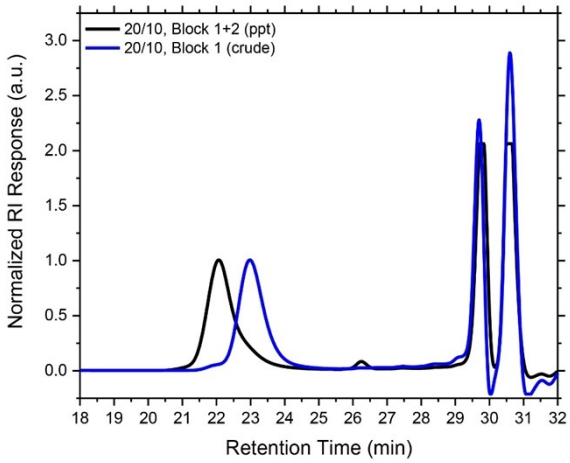

Figure S10: GPC traces illustrating the increase in molecular weight upon chain extension of the first block (containing just the **MePh** monomer) to create the Boc-protected copolymer (**MePh$_{20}$-*b*-dG$_{10}$**), shown here after purification by precipitation.

MePh$_{30}$-*b*-dG$_{15}$: ^{1}H NMR (500 MHz, CD_3CN) δ 11.53 (br, 2H), 8.35 (br, 2H), 7.33 (br, 10H), 5.83 (*trans*) and 5.58 (*cis*) (br, 6H total), 5.01 (br, 4H), 5.01 (*cis*) and 4.60 (*trans*) (br, 6H total), 4.16 (br, 4H), 3.55 (br, 4H), 3.46 (br, 6H), 3.13 (br, 6H), 1.47 (s, 18H), 1.41 (s, 18H).

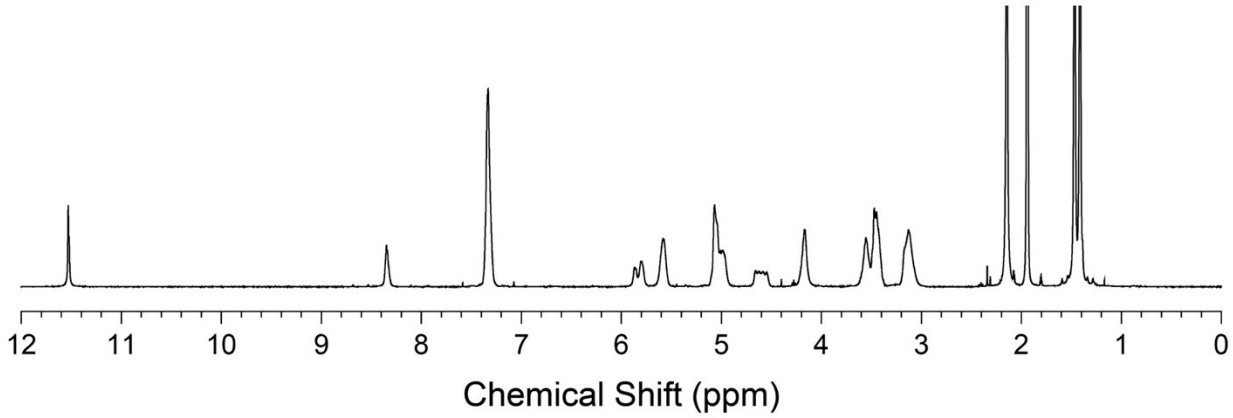

Figure S11: ^{1}H NMR spectrum in deuterated acetonitrile of the Boc-protected copolymer **MePh$_{30}$-*b*-dG$_{15}$** after purification by precipitation.

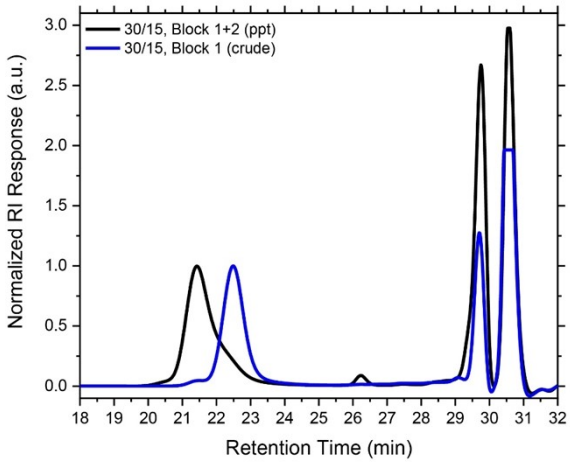

Figure S12: GPC traces illustrating the increase in molecular weight upon chain extension of the first block (containing just the **MePh** monomer) to create the Boc-protected copolymer (**MePh$_{30}$-*b*-dG$_{15}$**), shown here after purification by precipitation.

MePh$_{40}$-*b*-dG$_{20}$: ^{1}H NMR (500 MHz, CD_3CN) δ 11.53 (br, 2H), 8.35 (br, 2H), 7.33 (br, 10H), 5.83 (*trans*) and 5.58 (*cis*) (br, 6H total), 5.03 (br, 4H), 5.03 (*cis*) and 4.60 (*trans*) (br, 6H total), 4.17 (br, 4H), 3.55 (br, 4H), 3.46 (br, 6H), 3.13 (br, 6H), 1.47 (s, 18H), 1.41 (s, 18H).

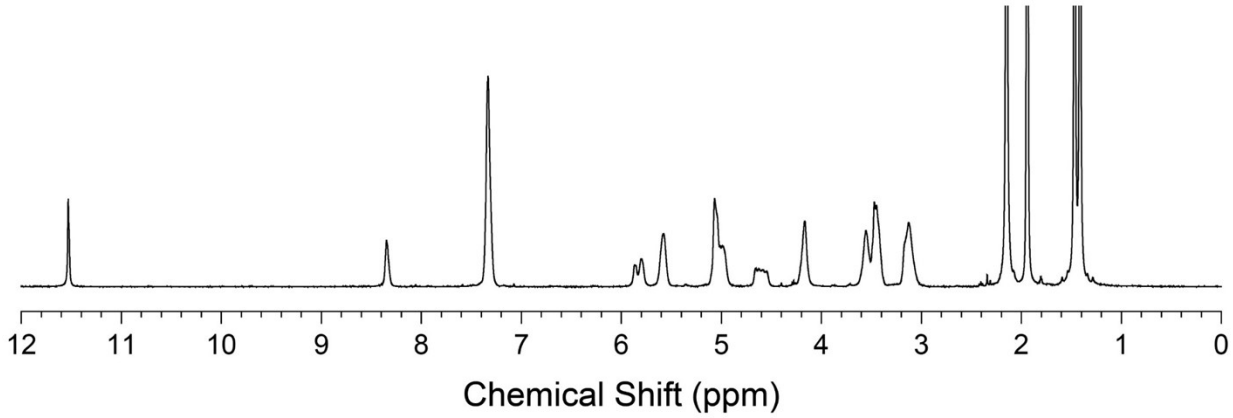

Figure S13: ^{1}H NMR spectrum in deuterated acetonitrile of the Boc-protected copolymer **MePh$_{40}$-*b*-dG$_{20}$** after purification by precipitation.

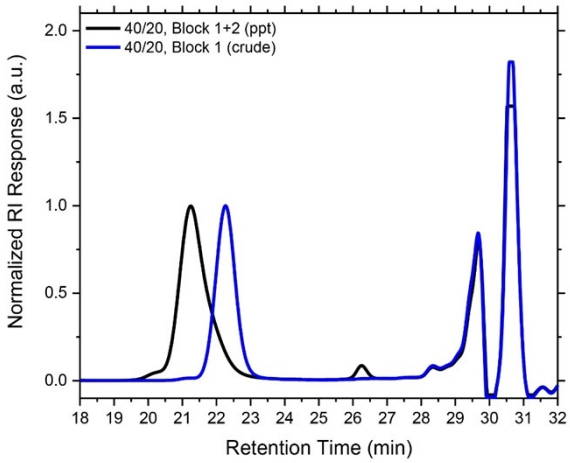

Figure S14: GPC traces illustrating the increase in molecular weight upon chain extension of the first block (containing just the **MePh** monomer) to create the Boc-protected copolymer (**MePh$_{40}$-*b*-dG$_{20}$**), shown here after purification by precipitation.

MePh$_{80}$-*b*-dG$_{40}$: ^{1}H NMR (500 MHz, CD_3CN) δ 11.53 (br, 2H), 8.35 (br, 2H), 7.33 (br, 10H), 5.84 (*trans*) and 5.58 (*cis*) (br, 6H total), 5.01 (br, 4H), 5.01 (*cis*) and 4.60 (*trans*) (br, 6H total), 4.17 (br, 4H), 3.61 (br, 4H), 3.46 (br, 6H), 3.15 (br, 6H), 1.48 (s, 18H), 1.42 (s, 18H).

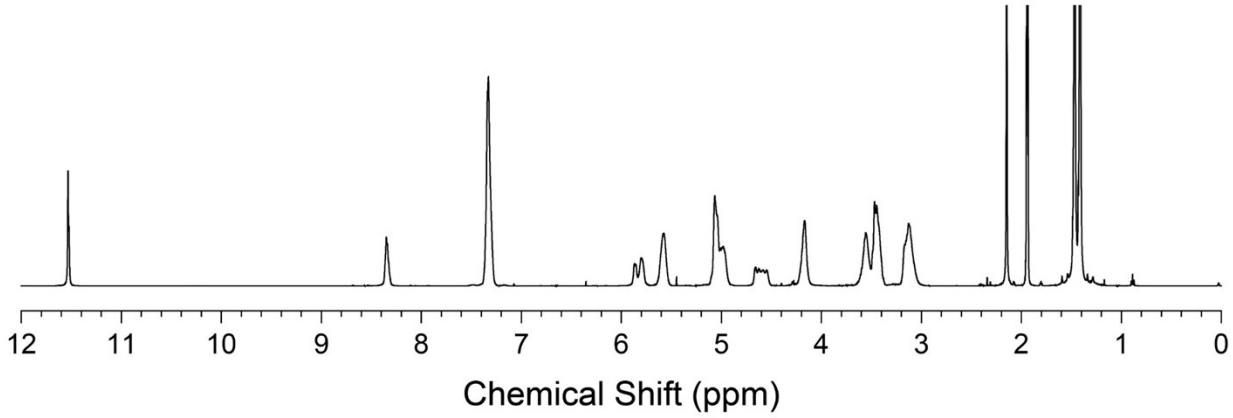

Figure S15: ^{1}H NMR spectrum in deuterated acetonitrile of the Boc-protected copolymer **MePh$_{80}$-*b*-dG$_{40}$** after purification by precipitation.

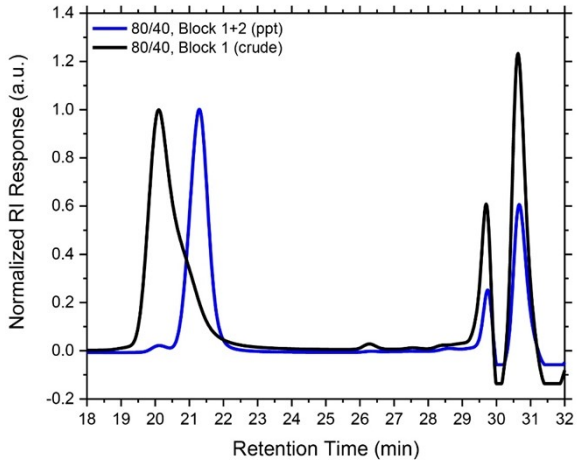

Figure S16: GPC traces illustrating the increase in molecular weight upon chain extension of the first block (containing just the **MePh** monomer) to create the Boc-protected copolymer (**MePh$_{80}$-*b*-dG$_{40}$**), shown here after purification by precipitation.

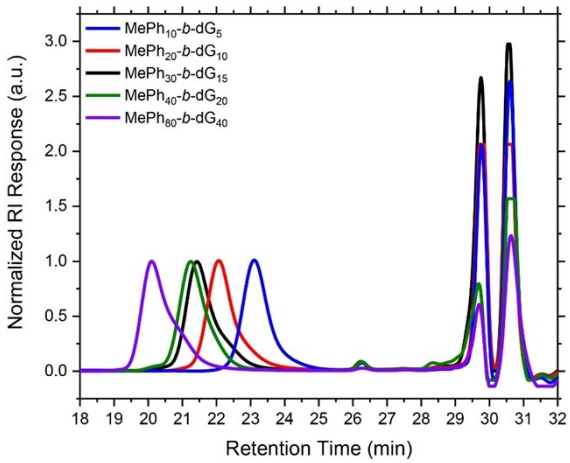

Figure S17: Overlay of all GPC traces for the purified, Boc-protected polymers in the **MePh$_{2n}$-*b*-dG$_{n}$** series, illustrating the differences in molecular weight distributions obtained.

3. Polymer Deprotection

To remove the Boc protecting groups, each polymer was dissolved in a 4 mL solution of 1:1 CH_2Cl_2:trifluoroacetic acid (TFA) and stirred in a scintillation vial overnight. The scintillation vials were then filled to halfway with methanol and concentrated using rotary evaporation. This process was repeated up to 7 times to remove traces of TFA by azeotropic distillation. The deprotected polymers were then dissolved in a minimal volume of methanol, diluted in approximately 10 mL of reverse osmosis (RO) water, and loaded into hydrated dialysis membrane tubing (MWCO = 500-1000 Da). All polymers were dialyzed against RO water until the conductivity of the solution outside the bag reached 0.3 μS or lower. Once dialysis was completed, polymer solutions were flash frozen in plastic cups by submerging them in liquid nitrogen. Frozen water was then removed by lyophilization *in vacuo* over the course of 3-5 days. ^{1}H NMR was used to confirm complete removal of the Boc groups to yield the deprotected guanidinium functional groups.

B. Protein Delivery

1. Homopolymer-Mediated EGFP Delivery

EGFP delivery followed previously published protocols.[5–11] PTDMs were dissolved in DMSO to make 1 mM stock solutions and stored at -20 °C. Jurkat T cells were harvested on the day of the experiment and seeded in 12-well plates at a density of 4 x 10^5 cells/0.8 mL of fresh serum-containing RPMI (800 μL per well). Stock EGFP (1 mg/mL) was diluted 1:21 in 1X phosphate-buffered saline (PBS, pH ~7.4) to make a less concentrated working solution. Polymer stock solutions were diluted 1:20 in PBS to create working solutions of 50 μM. Polymer:protein complexes were prepared by combining appropriate volumes of PBS, EGFP, and PTDM (in that order) to achieve 200 μL solutions whose final delivery concentrations (after combining with the

0.8 mL cell solutions in a later step) were 60 nM EGFP and 1.2, 0.6, or 0.3 μM PTDM (*n* = 20 ,40, or 80, respectively). Resulting molar ratios of PTDM:protein were thus 20:1, 10:1, or 5:1, respectively. Inequal polymer:protein ratios were selected in order to maintain equivalent polymer repeat unit:protein ratios (400:1) across all samples, successfully isolating the effect of increased monomer connectivity on delivery. Thus, while molar concentration was varied based on PTDM DP, weight concentration remained at ~14 μg/mL $\mathbf{dG}_n$ or ~0.9 μg/mL $\mathbf{PGON}_n$ regardless of PTDM DP. The solutions were incubated in the dark at room temperature for 30 minutes to allow complexation, then added dropwise to each well containing cells, resulting in final delivery volumes of 1 mL. The cells were incubated with the complexes for 4 h at 37 ℃ in 5% CO_2. After the incubation period, the cells were harvested, transferred to microcentrifuge tubes, collected by centrifugation for 5 min at 400 x *g*, and washed 3 times with 800 μL heparin (20 U/mL in PBS) to remove any extracellular or surface-bound complexes, in accordance with previously published procedures.[12] Cells were resuspended in 200 μL of FACS buffer (0.2% [w/w] bovine serum albumin in PBS) containing 2.5% (v/v) of 7-aminoactinomycin D (7-AAD) stain prior to internalization and viability analysis by flow cytometry, in which data for 10,000 cells were collected.

2. Block Copolymer-Mediated EGFP Delivery

Block copolymer-mediated EGFP delivery was performed in an identical manner to the above-described homopolymer-mediated EGFP delivery with the following modifications. Stock EGFP (1 mg/mL) was diluted 1:37 in PBS to achieve an appropriate working solution. Polymer stock solutions (1 mM) were diluted in 1:10 in PBS to achieve working solutions of 100 μM. Final delivery concentrations were 50 nM EGFP and 2, 0.5, or 0.25 μM PTDM (*2n*/*n* = 10/5, 40/20, and 80/40, respectively). Resulting molar ratios of PTDM:protein were thus 40:1, 10:1, and 5:1,

respectively. Inequal polymer:protein ratios were selected in order to maintain equivalent polymer repeat unit:protein ratios (600:1) across all samples, successfully isolating the effect of increased monomer connectivity on delivery. Thus, while molar concentration was varied based on PTDM DP, weight concentration remained at ~12 μg/mL **MePh$_{2n}$-*b*-dG$_n$** regardless of PTDM DP.

3. Block Copolymer-Mediated IgG Delivery in Jurkat T Cells

Block copolymer-mediated IgG-AF488 delivery in Jurkat T cells was performed in an identical manner to the above-described homopolymer-mediated EGFP delivery (substituting IgG for EGFP) with the following modifications. Stock IgG was received as 2 mg/mL and diluted 1:20 in PBS to make a working solution of 0.1 mg/mL. Polymer stock solutions (1 mM) were diluted 1:50 in PBS to make working solutions of 20 μM. Final delivery concentrations were 50 nM IgG-AF488 and 1, 0.5, 0.333, 0.25, or 0.125 μM PTDM (*2n*/*n* = 10/5, 20/10, 30/15, 40/20, and 80/40, respectively). Resulting molar ratios of PTDM:protein were thus 20:1, 10:1, 6.7:1, 5:1, and 2.5:1, respectively. Inequal polymer:protein ratios were selected in order to maintain equivalent polymer repeat unit:protein ratios (300:1) across all samples, successfully isolating the effect of increased monomer connectivity on delivery. Thus, while molar concentration was varied based on PTDM DP, weight concentration remained at ~6 μg/mL **MePh$_{2n}$-*b*-dG$_n$** regardless of PTDM DP.

4. Block Copolymer-Mediated IgG Delivery in mHippoE-18 Cells

Block copolymer-mediated IgG-AF488 delivery in mHippoE-18 cells was performed in an identical manner to the above-described homopolymer-mediated EGFP delivery (substituting IgG for EGFP) with the following modifications. mHippoE cells were harvested 24 h prior to the experiment and seeded in 12-well plates at a density of 7.5 x 10^4 cells/well. Stock IgG (2 mg/mL) was diluted 1:1000 in PBS to achieve a working concentration of 0.1 μM. Polymer stock solutions (1 mM) were serially diluted 1:10,000 in PBS to achieve 100 nM working concentrations. Final

delivery concentrations were 1 nM IgG-AF488 and 5, 2.5, 1.667, or 1.25 nM PTDM (*2n*/*n* = 10/5, 20/10, 30/15, and 40/20, respectively). Resulting molar ratios of PTDM:protein were thus 5:1, 3:1, 2:1, and 1:.25:1, respectively. Inequal polymer:protein ratios were selected in order to maintain equivalent polymer repeat unit:protein ratios (75:1) across all samples, successfully isolating the effect of increased monomer connectivity on delivery. Thus, while molar concentration was varied based on PTDM DP, weight concentration remained at ~29 pg/mL **MePh$_{2n}$-*b*-dG$_n$** regardless of PTDM DP. Immediately prior to treatment with the complexes, the medium was aspirated from each well and replaced with 800 µL of fresh, serum-containing DMEM. Following the incubation period, the medium was aspirated from each well, and the cells were rinsed with PBS, lifted with 0.25% trypsin-EDTA, diluted with DMEM (5x volume of trypsin), and collected by centrifugation for 5 min at 400 x *g*. After washing with heparin, cells were resuspended in 100% FACS buffer (viability was not assessed in these experiments).

5. Cre Delivery: PTDM Molecular Weight Comparison

Block copolymer-mediated Cre delivery in Jurkat-GFP cells was performed in an identical manner to the above-described homopolymer-mediated EGFP delivery (substituting Cre for EGFP) with the following modifications. Jurkat-GFP cells were seeded in a 24-well plates at a density of 2 x 10^5 cells/0.4 mL (400 µL total) of serum-free RPMI. Stock Cre was received as 60 µM and diluted 1:24 in PBS to achieve a working concentration of 2.5 µM. Polymer stock solutions (1 mM) were diluted 1:64 in PBS to create working solutions. Complexes were prepared in volumes of 100 µL (0.5 mL final delivery volume) with final delivery concentrations of 125 nM Cre and 0.625, 0.313, 0.208, 0.156, or 0.078 µM PTDM (*2n*/*n* = 10/5, 20/10, 30/15, 40/20, and 80/40, respectively). Resulting molar ratios of PTDM:protein were thus 5:1, 2.5:1, 1.667:1, 1.25:1, and 0.625:1, respectively. Inequal polymer:protein ratios were selected in order to maintain equivalent polymer

repeat unit:protein ratios (75:1) across all samples, successfully isolating the effect of increased monomer connectivity on delivery. Thus, while molar concentration was varied based on PTDM DP, weight concentration remained at 3.6 ng/mL **MePh$_{2n}$-*b*-dG$_n$** regardless of PTDM DP. Halfway through the 4h incubation of complexes with cells, 500 µL of serum-containing RPMI was added on top of wells to aid with cellular viability. At the end of the incubation, 10 µL was taken from each well, stained with trypan blue, and counted on a hemocytometer to assess cellular viability. The remainder of the sample was centrifuged for 5 min at 400 x *g*, resuspended in fresh serum-containing RPMI, and replated. The cells were cultured for 5 days, at which point they were harvested by centrifugation and washed once with PBS. Cells were then directly stained with 7-AAD to exclude dead cells from analysis during flow cytometry.

6. Cre Delivery: PTDM Molar Ratio Comparison

Block copolymer-mediated Cre delivery in Jurkat-GFP cells was performed in an identical manner to the above-described Cre molecular weight comparison experiment with the following modifications. **MePh$_{2n}$-*b*-dG$_n$** polymers were used at PTDM:Cre molar ratios of 0.625:1, 1.25:1, 2.5:1, and 5:1 (0.078, 0.156, 0.313, and 0.625 µM, respectively, for *2n*/*n* = 10/5, 20/10, 30/15, 40/20, and 80/40). These molar concentrations were selected such that the highest ratio (5:1) of **MePh$_{10}$-*b*-dG$_5$** had approximately the same weight concentration (~3.6 ng/mL) of polymer as the lowest ratio (0.625:1) of **MePh$_{80}$-*b*-dG$_{40}$**, as in the molecular weight comparison experiments.

C. Dynamic Light Scattering

Dynamic light scattering measurement procedures were adapted from a previously published report.[13] Prior to polymer:protein complexation, all microcentrifuge vials (used to prepare solutions) and cuvettes were rinsed 3 times with filtered methanol and allowed to dry in a covered

box that allowed for filtered air to pass through. Cuvettes and microcentrifuge vials were allowed to dry up to overnight to ensure complete drying and prevent dust accumulation.

Measurements were collected for solutions containing PTDM:protein complexes in 1x PBS. Protein concentrations were held constant at 50 nM and 125 nM for IgG and Cre, respectively. For experiments examining the effect of PTDM DP on complex size, **MePh$_{2n}$-*b*-dG$_n$** polymers were used at molar ratios of PTDM:IgG = 20:1, 10:1, 6.67:1, 5:1, and 2.5:1 and PTDM:Cre ratios = 5:1, 2.5:1, 1.67:1, 1.25:1, and 0.625:1 for $2n/n$ = 10/5, 20/10, 30/15, 40/20, and 80/40, respectively. For experiments examining the effect of PTDM:protein ratio on complex size, additional samples were prepared at molar ratios of PTDM:IgG = 2.5:1 and 20:1 for $2n/n$ = 10/5 and 80/40, respectively.

For IgG DLS samples, 1 mM stock solutions of PTDM were prepared by dissolving solid polymer in DMSO that had been filtered through 0.45 μM PES filters. 1x PBS was then filtered through 0.45 μM PES filters and subsequently used to prepare working solutions of both PTDM (10 μM) and protein. Appropriate volumes of PTDM and protein were then combined in 1.5 mL microcentrifuge tubes containing appropriate volumes of 1x PBS to achieve the final desired concentrations. Samples were mixed by gently pipetting up and down, incubated for 30 min at room temperature to allow complexes to form, and then carefully transferred to polystyrene cuvettes for analysis.

For Cre DLS samples, PTDM stock solutions were prepared in DMSO that had not been filtered previously, though filtered 1x PBS was used to create working solutions of both PTDM and Cre. Samples were prepared directly in cuvettes, mixed by gently pipetting up and down, and then covered with a small slip of aluminum foil for 30 min prior to analysis.

It is important to note that the assumed RI value used in the SOP and absorbance of the material were used to convert the raw intensity-based size data to the number-based size data which have been reported in the main text. The distribution most closely related to the raw data is the intensity data, though the trends reported can be observed in either the intensity- or number-based analysis of particle size.

D. Fluorescence-Based Equilibrium Binding Assays

To isolate the effect of increasing PTDM degree of polymerization on protein binding, equilibrium fluorescence quenching assays were conducted according to previously published procedures using BSA-FITC as a model cargo.[5,8,10] These assays were conducted at 25 °C in 1x PBS at pH ~7.2, and the fluorescence of BSA-FITC was monitored and recorded as a function of increasing PTDM concentration from 0 to 8 μM (corresponding to ~ 47, 94, 140, and 186 mg/mL for the *2n*/*n* = 10/5, 20/10, 30/15, and 40/20 polymers, respectively). These experiments were conducted in a 96-well polystyrene plate, where each well had black opaque sides and flat clear bottoms. In general, each well in the titration was designed to contain 200 nM BSA-FITC, the appropriate carrier concentration, and PBS to reach a total volume of 200 μL. A stock solution of 1 mg/mL BSA-FITC in 1x PBS was prepared and used to prepare more dilute working solutions of dye-labelled protein. PTDM stock concentrations of 1 mM in pure DMSO were serially diluted in PBS to obtain working solutions of 100 μM (10% v/v DMSO) and 10 μM (1% v/v DMSO. Variable volumes from these working solutions were added to the wells such that each subsequent well in the series contained an increasing final concentration of carrier. Since the use of different carrier stock solutions introduced DMSO in varying amounts, additional volumes of pure DMSO were added to each well such that all wells contained the same final concentration (v/v) of DMSO. Once all wells had received the appropriate volumes of PBS, BSA-FITC, DMSO, and PTDM, in that

order, they were gently mixed by pipetting up and down and stirring with the tip of the pipet. The 96-well plate was incubated in the dark (covered by the plastic lid and under foil) at room temperature for 30 min to achieve equilibrium prior to fluorescence measurements. Samples were excited at 495 nm and emission was read at 523 nm with a BioTek Mx plate reader. During the binding experiments, the fluorescence intensity of each well in the titration was measured. The background fluorescence of a negative control (containing only PBS and the appropriate DMSO concentration) was first subtracted from these measurements. Next, the values were normalized by the fluorescence intensity of a positive control (containing only 200 nM BSA-FITC in PBS and the appropriate DMSO concentration) to yield a plot of normalized FITC fluorescence intensity vs. PTDM concentration. The binding experiments were repeated in triplicate for each PTDM. In certain cases, follow-up experiments consisting of three additional replicates at additional PTDM concentrations were performed in order to provide more data in critical regions of the binding curves.

III. Supplemental Data

A. IgG-AF488 Delivery in mHippoE-18 Cells

Delivery of IgG-AF488 was replicated in the embryonic mouse hippocampal-18 (mHippoE-18) cell line as an indicator of whether trends observed in Jurkat T cells (i.e., higher uptake with shorter polymers) might be more broadly applicable to other cell types (Figure S18).

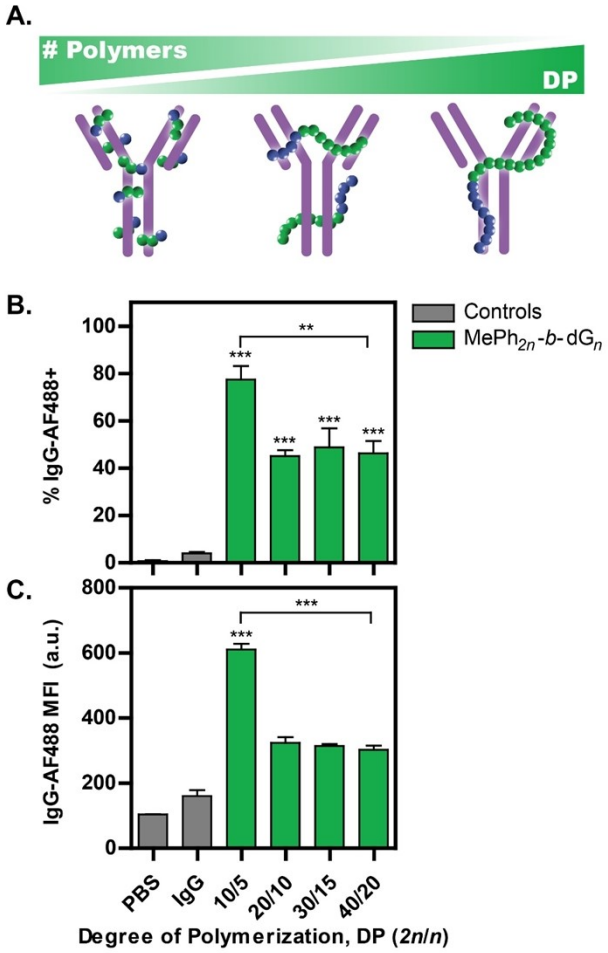

Figure S18: AlexaFluor (AF)488 conjugated IgG internalization in embryonic mouse hippocampal-18 (mHippoE-18) cells as a function of PTDM degree of polymerization (DP). (A) Illustration of the inverse relationship between DP and number of polymer molecules in the system given that the total number of polymer repeat units in the system is universally conserved. As shorter polymers are linked together to form longer ones, fewer independent chains remain, allowing for a direct assessment of the impact of monomer connectivity on delivery. IgG internalization is quantified as (B) percentage of live cells positive for AF488 and (C) median fluorescence intensity (MFI) of the entire live-cell population. Data are displayed as the mean ± the standard error of the mean for four independent replicates of 10,000 cells each. Statistics indicate significance in comparison with the PBS and IgG controls (grey), unless otherwise noted: * = $p < 0.05$, ** = $p < 0.01$, *** = $p < 0.001$, no symbol (or ns) = no significance, as determined by one-way ANOVA followed by a Tukey post-test.

B. Flow Cytometry Histograms

Representative flow cytometry histograms to accompany the data found in Figure 2, Figure 3, Figure 4, Figure S18, Figure 5, and Figure 6 can be found in Figure S19, Figure S20, Figure S21, Figure S22, Figure S23, and Figure S24, respectively, below.

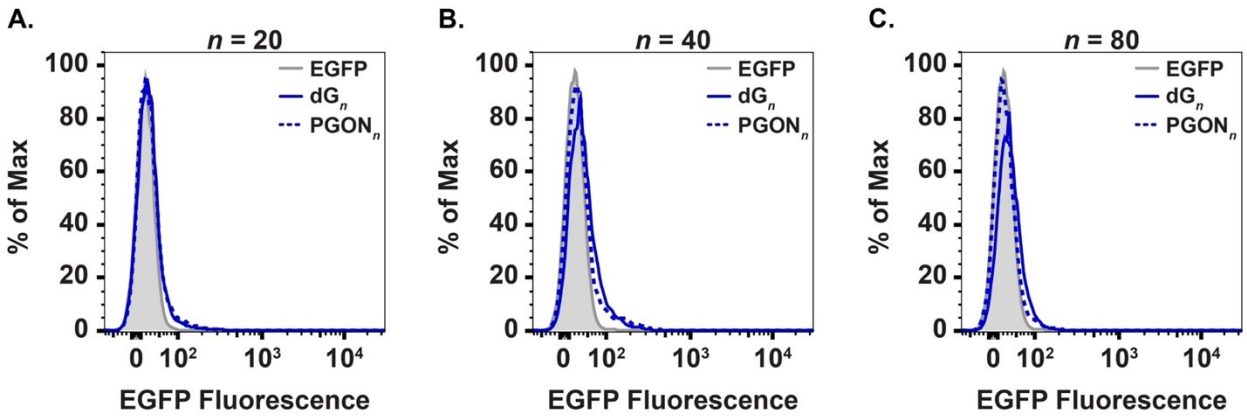

Figure S19: Representative flow cytometry histograms for delivery of EGFP into Jurkat T cells using homopolymers at degrees of polymerization of (A) 20, (B) 40, and (C) 80 to accompany the data presented in Figure 2 of the main text. Delivery with the **dG*n*** and **PGON*n*** series is indicated with a solid and dashed blue line, respectively, overlaid with the EGFP only control (shaded grey).

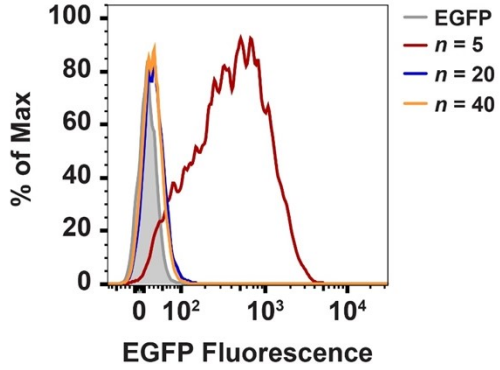

Figure S20: Representative flow cytometry histograms for delivery of EGFP into Jurkat T cells using the block copolymer series to accompany the data presented in Figure 3 of the main text. Delivery at *n* = 5, 20, and 40 is indicated with a solid red, blue, and yellow line, respectively, overlaid with the EGFP only control (shaded grey).

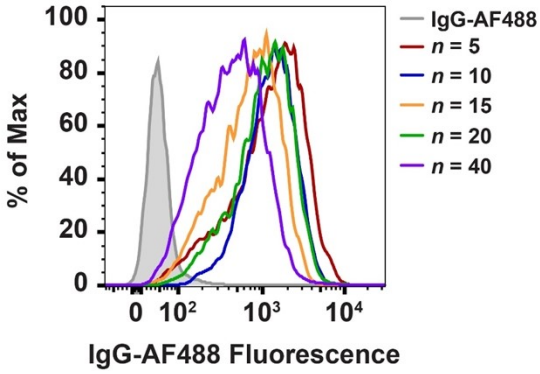

Figure S21: Representative flow cytometry histograms for delivery of IgG-AF488 into Jurkat T cells using the block copolymer series to accompany the data presented in Figure 4 of the main text. Delivery at *n* = 5, 10, 15, 20, and 40 is indicated with a solid red, blue, yellow, green, and purple line, respectively, overlaid with the IgG-AF488 only control (shaded grey).

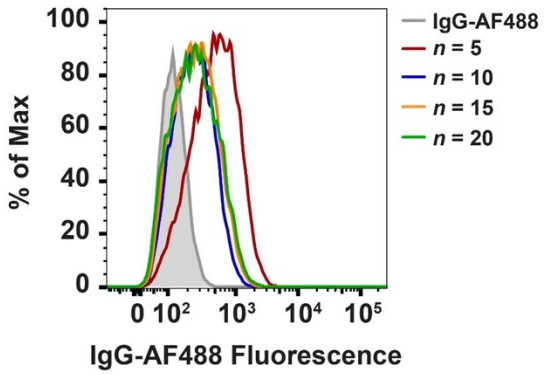

Figure S22: Representative flow cytometry histograms for delivery of IgG-AF488 into mHippoE cells using the block copolymer series to accompany the data presented in Figure S18. Delivery at n = 5, 10, 15, and 20 is indicated with a solid red, blue, yellow, and green line, respectively, overlaid with the IgG-AF488 only control (shaded grey).

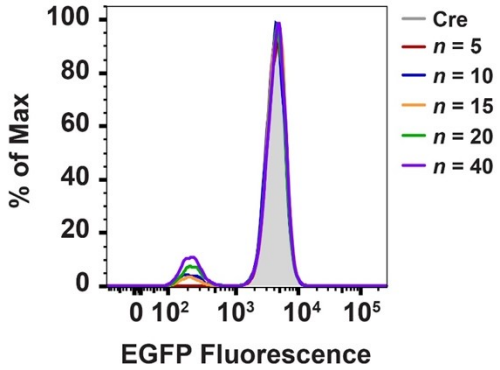

Figure S23: Representative flow cytometry histograms for delivery of Cre recombinase into a modified Jurkat T cell line (resulting in loss of EGFP fluorescence in the cell when successful) using the block copolymer series to accompany the data presented in Figure **S18** 5 of the main text. Delivery at n = 5, 10, 15, 20, and 40 is indicated with a solid red, blue, yellow, green, and purple line, respectively, overlaid with the Cre only control (shaded grey).

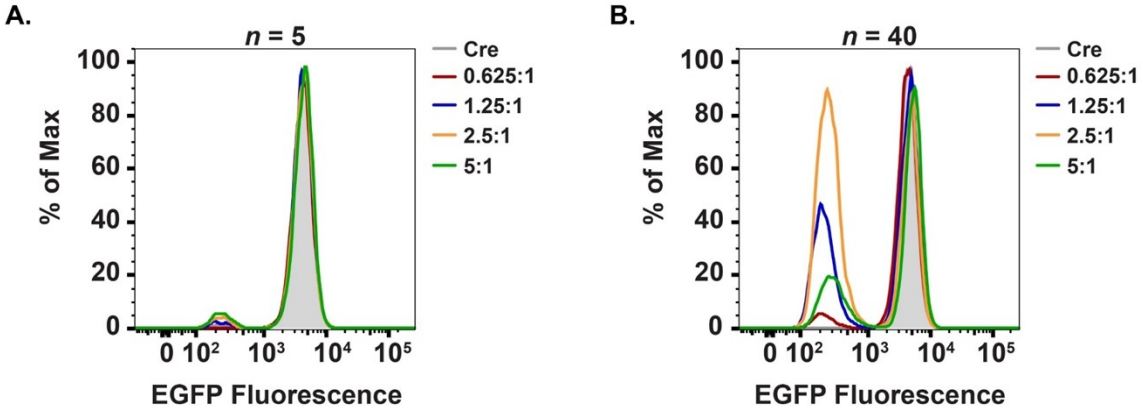

Figure S24: Representative flow cytometry histograms for delivery of Cre recombinase into a modified Jurkat T cell line (resulting in loss of EGFP fluorescence in the cell when successful) using (A) **MePh$_{10}$-*b*-dG$_5$** and (B) **MePh$_{80}$-*b*-dG$_5$** at various ratios to accompany the data presented in Figure **S18** 6 of the main text. Delivery at PTDM:Cre = 0.625:1, 1.25:1, 2.5:1, and 5:1 is indicated with a solid red, blue, yellow, and green, line, respectively, overlaid with the Cre only control (shaded grey).

C. Cellular Viability

7-AAD staining was used to assess viability in all of the delivery experiments in Jurkat and Jurkat-GFP cell lines (Figures 2-6). No significant cellular toxicity was observed for any of the experimental conditions in Figures 2-5 of the main text (Figure S25). In contrast, the highest concentrations of the longest block copolymer PTDM in the final experiment resulted in significant cellular death (Figure 6C in the main text).

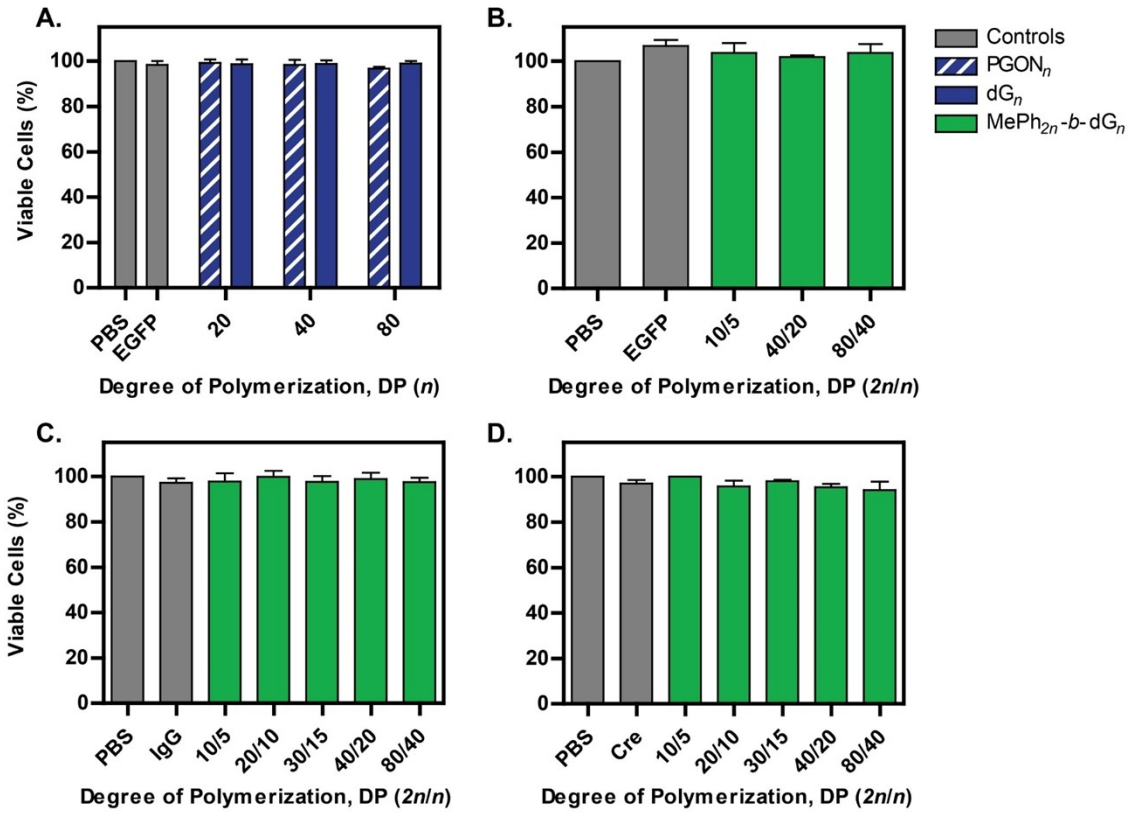

Figure S25: Cellular viability for EGFP (A-B), IgG (C), and Cre (D) delivery using PTDMs in the **PGON$_n$** (hatched blue bars), **dG$_n$** (solid blue bars), and **MePh$_{2n}$-*b*-dG$_n$** (solid green bars) series to accompany Figures 2-5 of the main text. Viability was determined by either 7-AAD (A-C) or trypan blue (D) staining immediately following delivery. 7-AAD data (A-C), obtained by flow cytometry, are displayed as the mean ± the standard error of the mean (SEM) for three (B) or four (A, C) independent replicates of 10,000 cells each. Trypan blue data (D), obtained by manual count with a hemocytometer, are displayed as the mean ± the SEM for three independent replicates. Statistical analyses of the datasets were done by one-way ANOVA followed by a Tukey post-test. For all samples, p values were > 0.05 when compared to their respective PBS and EGFP controls (grey).

D. Impact of Block Copolymer Length on Binding

BSA-FITC was used as a model fluorescent cargo to study the binding behavior of PTDMs as degree of polymerization was increased (Figure S26). Given that the binding regions of the curves (initial negative slope) collapsed onto each other when plotted by weight concentration (Figure S26B), but not when plotted by molar concentration (Figure S26A), it appears that total concentration of pendant functional groups (repeat units), rather than concentration of polymer chains, in the system is the main driving force behind PTDM:protein binding. It is interesting to note that after fluorescence quenching (i.e., binding) is achieved, the addition of more polymer into the system results in return of cargo fluorescence for polymers longer than $2n/n = 10/5$. This phenomenon becomes progressively more pronounced as degree of polymerization increases. While it is not known whether this is due to a rearrangement event (e.g., cargo release, PTDM micellization, etc.), or simply an artifact of a smaller change in local fluorophore environment, these conditions are well above concentrations used in delivery experiments and have not been pursued in this study. Future studies may elucidate whether the more amphiphilic nature of these longer PTDMs results in self-assembly, for example micelle formation, above certain concentrations.

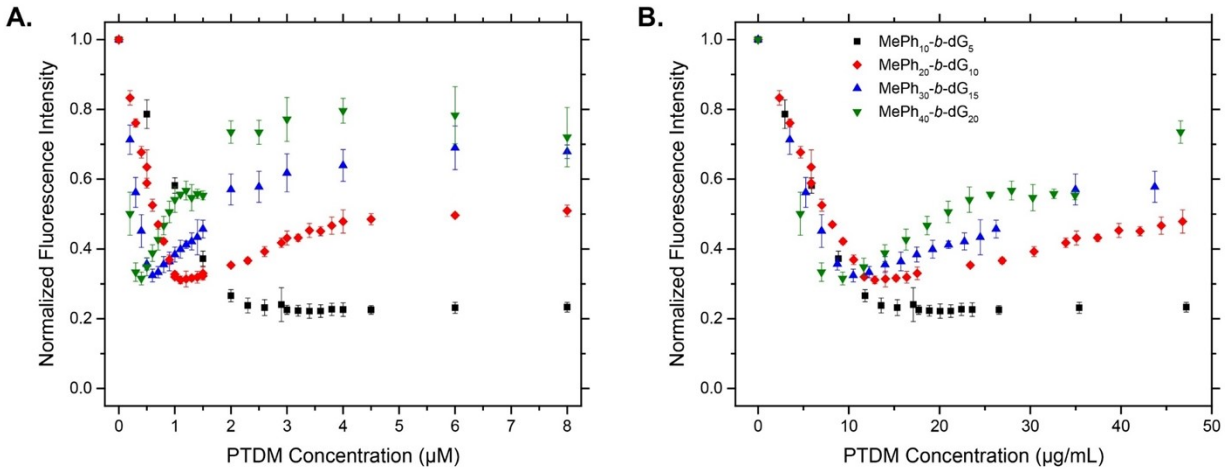

Figure S26: Fluorescence-quenching binding curves for PTDM:BSA-FITC pairs plotted by (A) PTDM molar concentration and (B) PTDM weight concentration. Replotting the data by weight concentration accounts for longer

PTDMs containing more pendant functional groups, essentially normalizing to isolate the effect of increasing the concentration of repeat units in the system. Data points represent the mean normalized fluorescence intensity from three independent replicates ± the standard deviation.

E. Particle Size by Dynamic Light Scattering

1. DLS of PTDM:IgG Complexes

The DLS data in Figure 7A and 7B of the main text were derived from the raw curves shown in Figure S27-SFigure **S28** and Figure S29-SFigure **S30**, respectively. Figure S27 and Figure S29 contain the intensity-based particle size distributions, while Figure S28 and Figure S30 display number-based population distributions. While the number distributions are of greater interest for the purposes of this study, it is important to recognize that they are derived directly from the intensity distributions using the estimated RI value entered in the SOP. Though redundant, plots for samples which were used to isolate the effects of both PTDM DP and PTDM:IgG molar ratio on particle size (i.e., **MePh$_{10}$-*b*-dG$_5$** at a ratio of 20:1 and **MePh$_{80}$-*b*-dG$_{40}$** at 2.5:1) have been included in both sets of figures for ease of comparison.

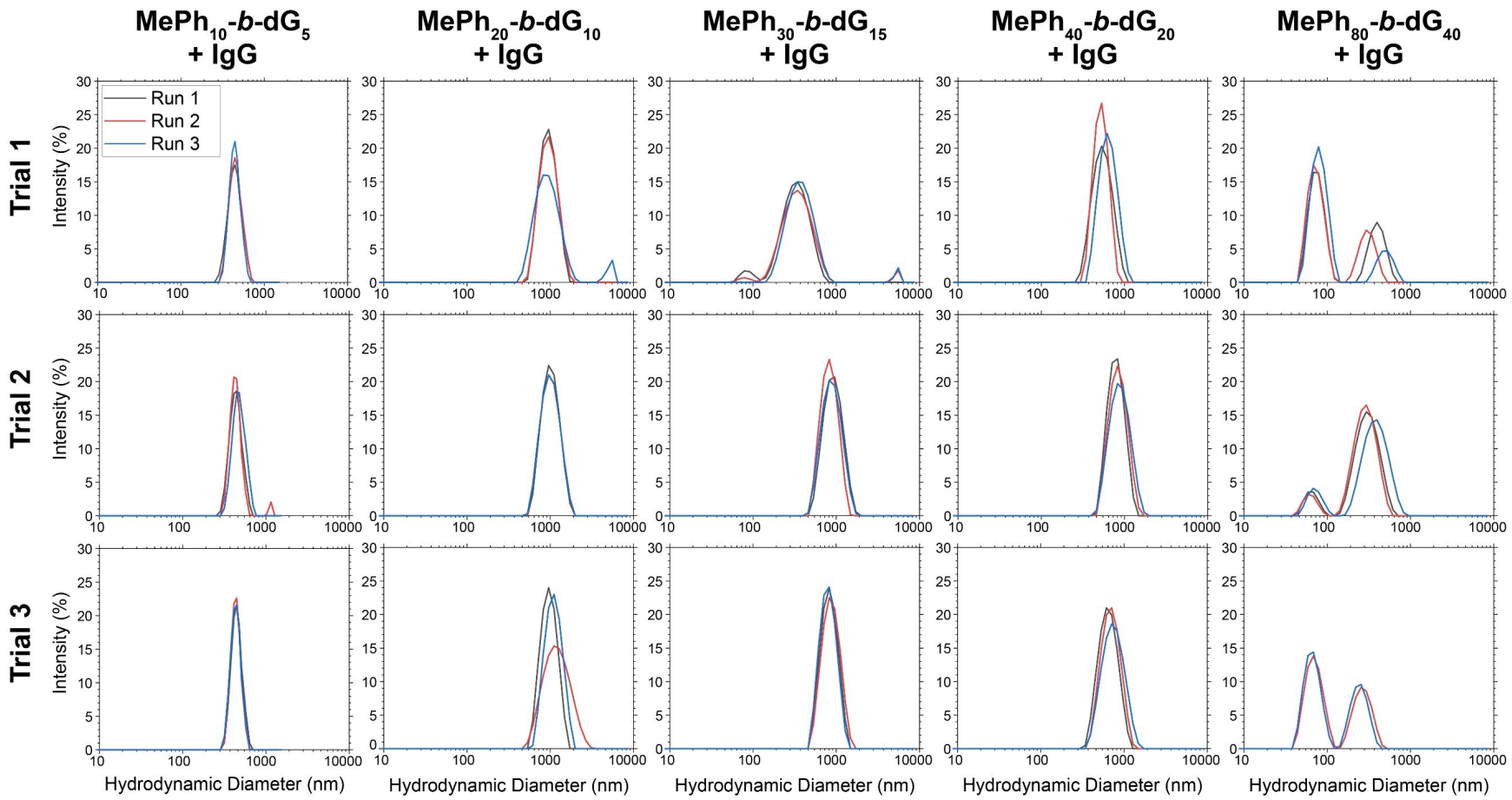

Figure S27: Raw DLS curves for **MePh$_{2n}$-*b*-dG$_n$**:IgG complexes plotted as percentage of total signal intensity as a function of diameter. Samples contained 50 nM IgG and PTDM:IgG molar ratios of 20:1, 10:1, 6.67:1, 5:1, and 2.5:1, respectively, for $2n/n$ = 10/5, 20/10, 30/15, 40/20, and 80/40. Each individual plot contains overlaid data from three scans of the same sample. One run with a poor correlation function (Trial 3, Run 1 of **MePh$_{80}$-*b*-dG$_{40}$**) has been omitted.

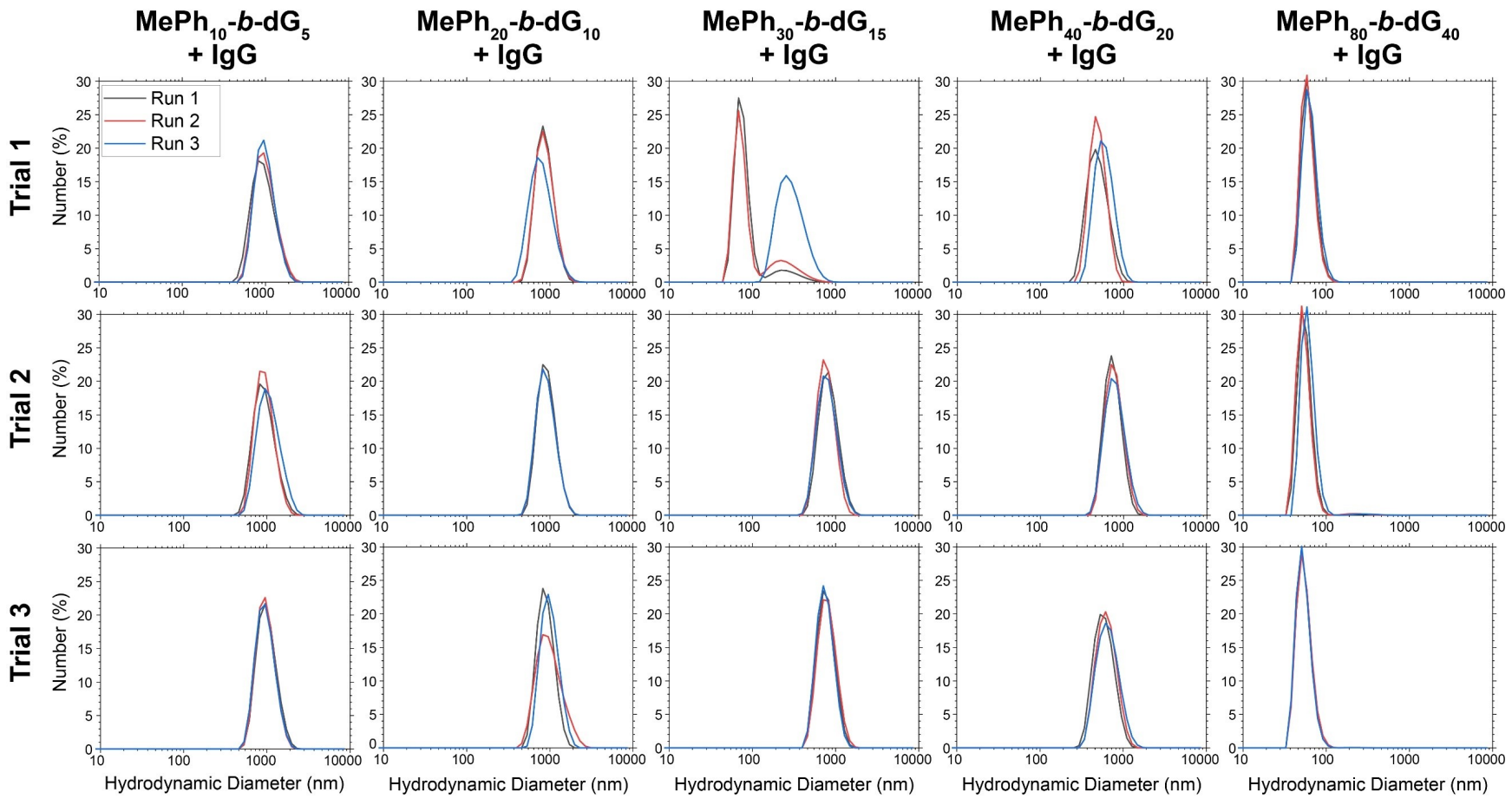

Figure S28: Raw DLS curves for **MePh$_{2n}$-*b*-dG$_n$**:IgG complexes plotted as percentage of total number of particles as a function of diameter. Samples contained 50 nM IgG and PTDM:IgG molar ratios of 20:1, 10:1, 6.67:1, 5:1, and 2.5:1, respectively, for *2n*/*n* = 10/5, 20/10, 30/15, 40/20, and 80/40. Each individual plot contains overlaid data from three scans of the same sample. One run with a poor correlation function (Trial 3, Run 1 of **MePh$_{80}$-*b*-dG$_{40}$**) has been omitted.

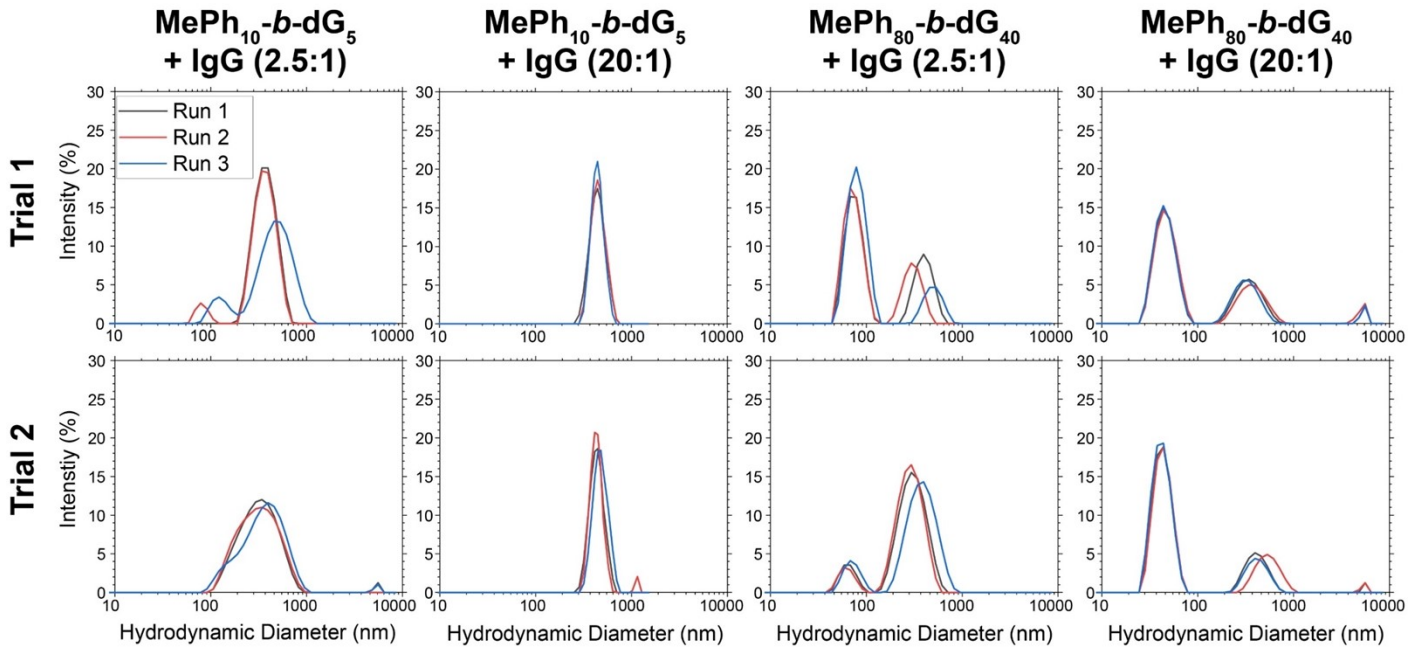

Figure S29: Raw DLS curves for **MePh$_{2n}$-*b*-dG$_n$**:IgG complexes plotted as percentage of total signal intensity as a function of diameter. Samples contained 50 nM IgG and various PTDM:IgG molar ratios as indicated at the top of each column. Each individual plot contains overlaid data from three scans of the same sample. Note that data contained within the middle two columns was included in Figure S27 but has been copied here for ease of comparison.

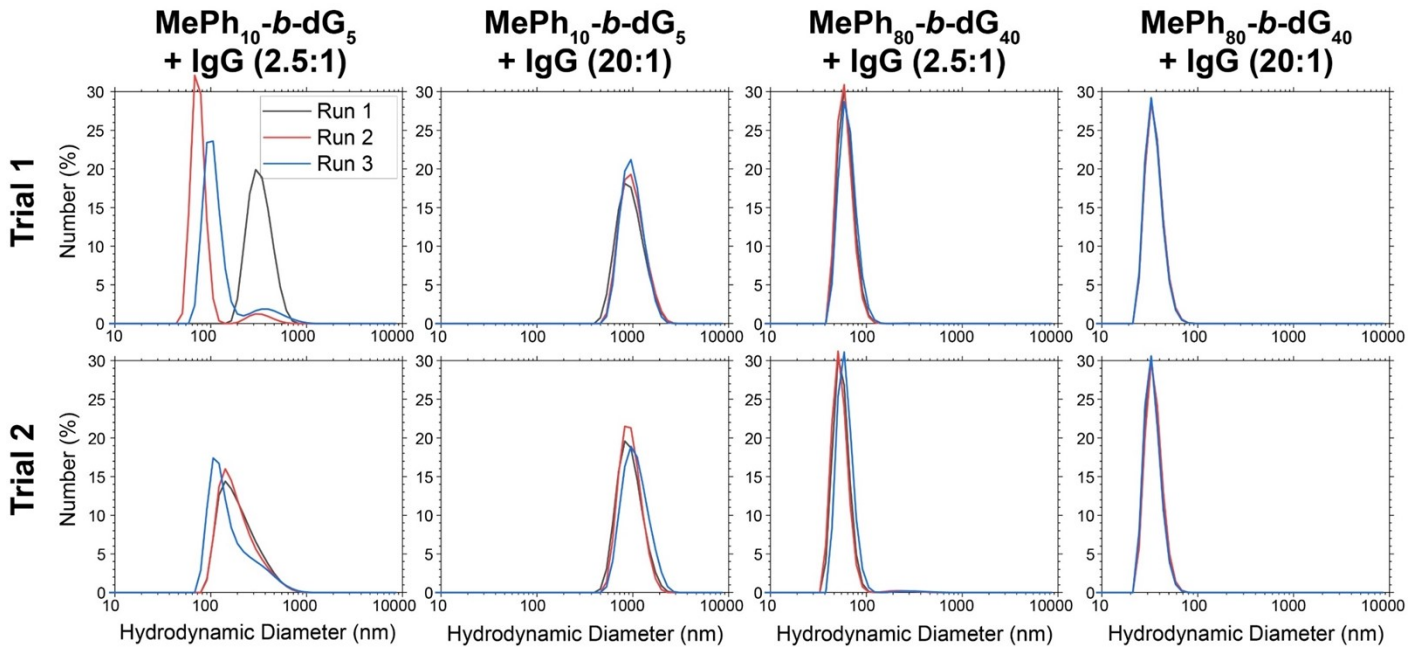

Figure S30: Raw DLS curves for **MePh$_{2n}$-*b*-dG$_n$**:IgG complexes plotted as percentage of total number of particles as a function of diameter. Samples contained 50 nM IgG and various PTDM:IgG molar ratios as indicated at the top of each column. Each individual plot contains overlaid data from three scans of the same sample. Note that data contained within the middle two columns was included in Figure S27 but has been copied here for ease of comparison.

2. DLS of PTDM:Cre Complexes

Given that PTDM:IgG complex size dramatically decreased with increasing polymer length, a similar experiment was conducted using PTDM:Cre complexes in order to probe whether this phenomenon extended to Cre and might provide insight into the differences in biological activity observed (Figure S31).

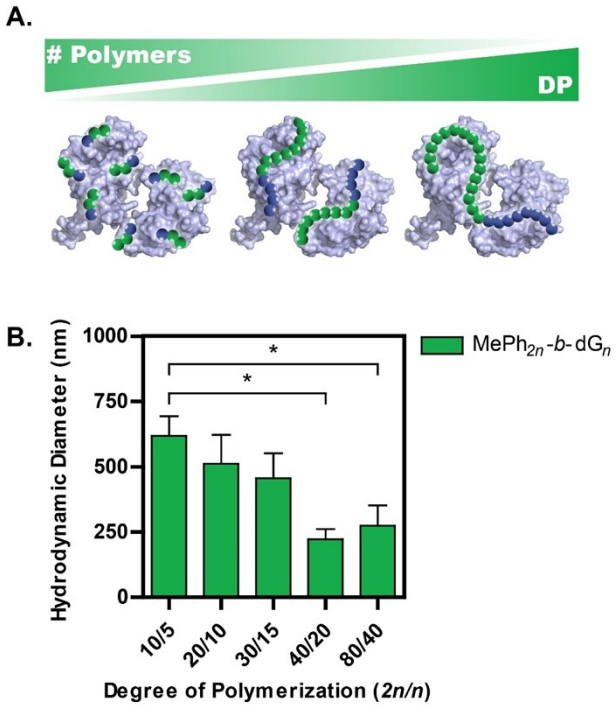

Figure S31: PTDM:Cre complex size as a function of PTDM degree of polymerization (DP). (A) Illustration of the inverse relationship between DP and number of polymer molecules in the system, given that the total number of polymer repeat units in the system is universally conserved. As shorter polymers are linked together to form longer ones, fewer independent chains remain, allowing for a direct assessment of the impact of monomer connectivity on complex size. (B) PTDM:Cre complex diameter as measured by dynamic light scattering (DLS) for increasing PTDM DP. Data are presented as the mean size (by number) of the most populous distribution (when multimodal) ± the standard deviation for three (C) independent replicates, each comprising three individual measurements of the same sample. In the case that a poor correlation curve was obtained, the measurement was omitted. Statistics indicate significance between the two data points indicated by brackets: * = $p < 0.05$, ** = $p < 0.01$, *** = $p < 0.001$, no symbol = no significance, as determined by one-way ANOVA followed by a Tukey post-test.

The raw intensity- and number-based particle size distributions from which Figure S31 was derived can be found in Figure S32 and Figure S33, respectively.

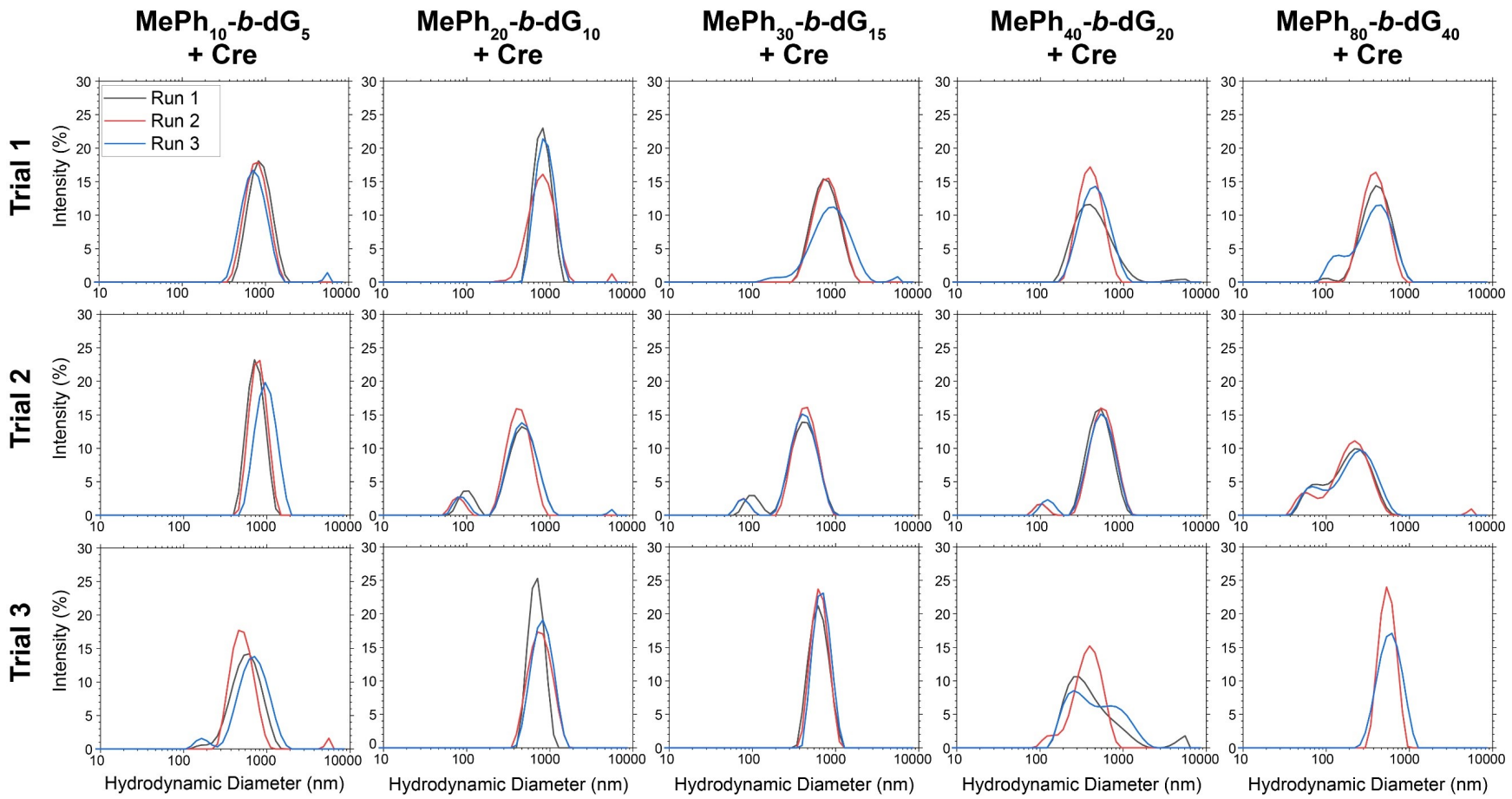

Figure S32: Raw DLS curves for **MePh$_{2n}$-*b*-dG$_n$**:Cre complexes plotted as percentage of total signal intensity as a function of diameter. Samples contained 125 nM Cre and PTDM:Cre molar ratios of 5:1, 2.5:1, 1.67:1, 1.25:1, and 0.625:1, respectively, for *2n*/*n* = 10/5, 20/10, 30/15, 40/20, and 80/40. Each individual plot contains overlaid data from three scans of the same sample. One run with a poor correlation function (Trial 1, Run 1 of **MePh$_{80}$-*b*-dG$_{40}$**) has been omitted.

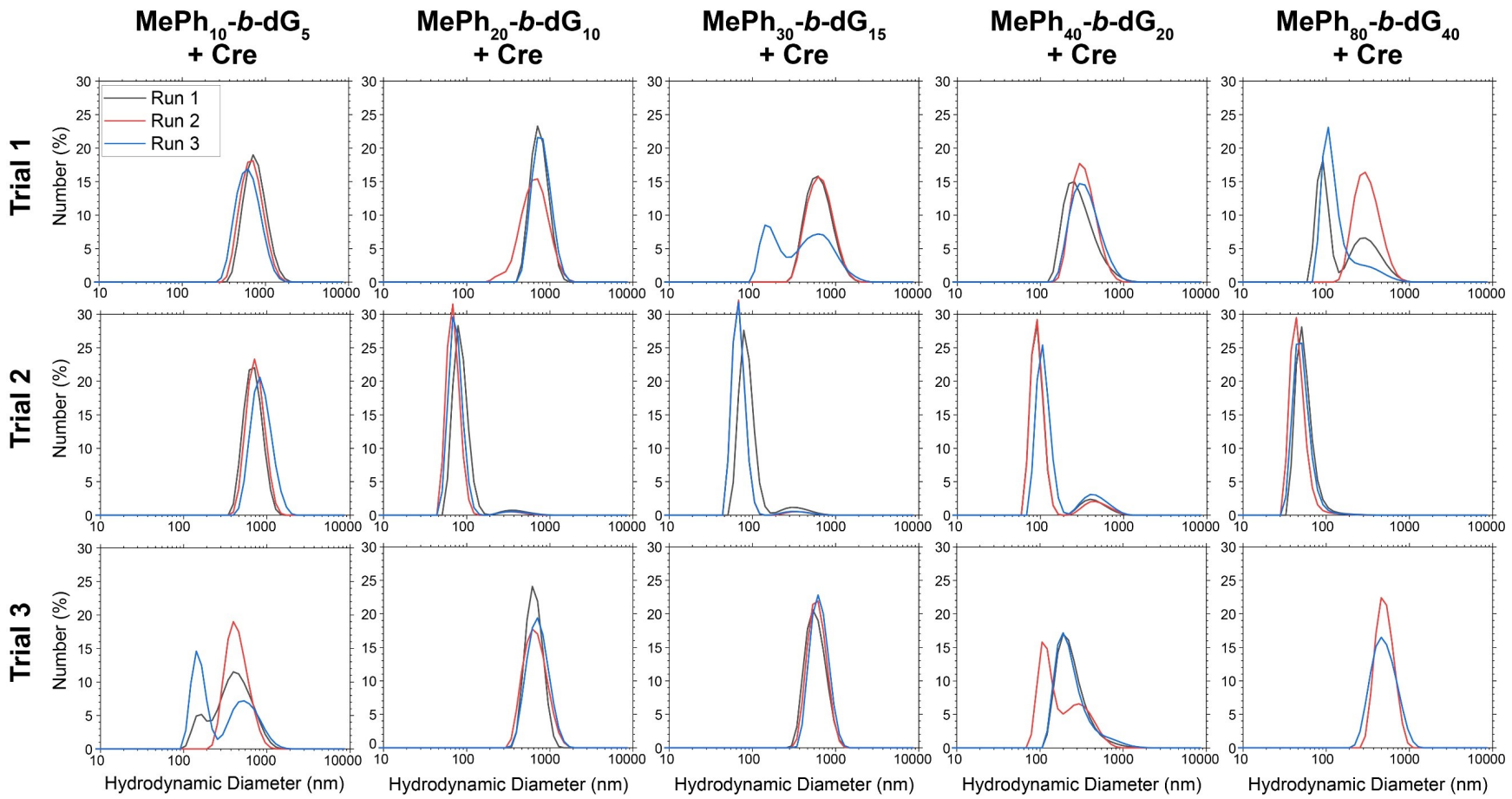

Figure S33: Raw DLS curves for **MePh$_{2n}$-*b*-dG$_n$**:Cre complexes plotted as percentage of total number of particles as a function of diameter. Samples contained 125 nM Cre and PTDM:Cre molar ratios of 5:1, 2.5:1, 1.67:1, 1.25:1, and 0.625:1, respectively, for *2n*/*n* = 10/5, 20/10, 30/15, 40/20, and 80/40. Each individual plot contains overlaid data from three scans of the same sample. One run with a poor correlation function (Trial 1, Run 1 of **MePh$_{80}$-*b*-dG$_{40}$**) has been omitted.

IV. References

(1) Love, J. A.; Morgan, J. P.; Trnka, T. M.; Grubbs, R. H. A Practical and Highly Active Ruthenium-Based Catalyst that Effects the Cross Metathesis of Acrylonitrile. *Angew. Chemie Int. Ed.* **2002**, *41* (21), 4035–4037.

(2) Caffrey, L. M.; deRonde, B. M.; Minter, L. M.; Tew, G. N. Mapping Optimal Charge Density and Length of ROMP-Based PTDMs for siRNA Internalization. *Biomacromolecules* **2016**, *17* (10), 3205–3212.

(3) deRonde, B. M.; Torres, J. A.; Minter, L. M.; Tew, G. N. Development of Guanidinium-Rich Protein Mimics for Efficient siRNA Delivery into Human T Cells. *Biomacromolecules* **2015**, *16* (10), 3172–3179.

(4) Lienkamp, K.; Madkour, A. E.; Musante, A.; Nelson, C. F.; Nüsslein, K.; Tew, G. N. Antimicrobial Polymers Prepared by ROMP with Unprecedented Selectivity: A Molecular Construction Kit Approach. *J. Am. Chem. Soc.* **2008**, *130* (30), 9836–9843.

(5) Posey, N. D.; Hango, C. R.; Minter, L. M.; Tew, G. N. The Role of Cargo Binding Strength in Polymer-Mediated Intracellular Protein Delivery. *Bioconjug. Chem.* **2018**, *29* (8), 2679–2690.

(6) Backlund, C. M.; Sgolastra, F.; Otter, R.; Minter, L. M.; Takeuchi, T.; Futaki, S.; Tew, G. N. Increased hydrophobic block length of PTDMs promotes protein internalization. *Polym. Chem.* **2016**, *7* (48), 7514–7521.

(7) Backlund, C. M.; Takeuchi, T.; Futaki, S.; Tew, G. N. Relating structure and internalization for ROMP-based protein mimics. *Biochim. Biophys. Acta - Biomembr.* **2016**, *1858* (7), 1443–1450.

(8) Sgolastra, F.; Backlund, C. M.; Ilker Ozay, E.; deRonde, B. M.; Minter, L. M.; Tew, G. N. Sequence segregation improves non-covalent protein delivery. *J. Control. Release* **2017**, *254*, 131–136.

(9) Tezgel, A. Ö.; Jacobs, P.; Backlund, C. M.; Telfer, J. C.; Tew, G. N. Synthetic Protein Mimics for Functional Protein Delivery. *Biomacromolecules* **2017**, *18* (3), 819–825.

(10) Posey, N. D.; Caffrey, L. M.; Minter, L. M.; Tew, G. N. Protein Mimic Hydrophobicity Affects Intracellular Delivery but not Cargo Binding. *ChemistrySelect* **2016**, *1* (19), 6146–6150.

(11) Backlund, C. M.; Hango, C. R.; Minter, L. M.; Tew, G. N. Protein and Antibody Delivery into Difficult-to-Transfect Cells by Polymeric Peptide Mimics. *ACS Appl. Bio Mater.* **2020**, *3* (1), 180–185.

(12) McNaughton, B. R.; Cronican, J. J.; Thompson, D. B.; Liu, D. R. Mammalian cell penetration, siRNA transfection, and DNA transfection by supercharged proteins. *Proc. Natl. Acad. Sci.* **2009**, *106* (15), 6111–6116.

(13) Posey, N. D.; Tew, G. N. Protein Transduction Domain Mimic (PTDM) Self-Assembly? *Polymers* **2018**, *10* (9), 1039.